Discussion of Big-picture Topics, followed by the individual reviews and our responses.

"climatology"

This appears to be a loaded word, and we have used it too carelessly. We have shifted a lot of "climatology(ies)" to "statistics" as recommended, but some use of the word is retained since it is the intent to build such a climatology. Thus the title has been changed to "building a climatology." The models are tested as to the robustness of their statistics in terms of space, but we did not go back and ask for full resubmissions with different years. We have previously shown that sampling along a single meridian in the tropical Pacific produces a robust 2D distribution of chemical species (see Fig 8 below from the Prather et al: Atmos. Chem. Phys., 17, 9081–9102, 2017, https://doi.org/10.5194/acp-17-9081-2017), and have added a simple test here by splitting the tropical Pacific block into east and west halves.

ATom-1 deployment only:

One review was critical on the choice of dates and wished to put the "first deployment" with dates in the title. We tried several versions and it was just too clumsy, and not really title material. Thus we have brought forward in the abstract and paper the fact that we are only presenting ATom-1 data. The dates are now specific: the ATom-1 deployment consisting of 10 research flights was 29 Jul to 23 Aug 2016. While the full ATom-1 measurements of J-cloudy and J-clear are reported and archived with this paper, we analyze here only the Pacific data north of 20ºS, which includes research flights 1-5 (29-Jul to 8-Aug). Likewise, the current model analysis includes only the two Pacific blocks from 20ºS to 50ºN, but the archived model data is global and for a mid-August day (varying years). Thus, later analyses can look at the Southern or Atlantic Oceans (or continental data) using the archived data sets.

Sampling of different years, more extensive cloud statistics, repeatability of just one day in August:

We agree with reviewer Collins that it would be wonderful to have done this analysis for the full month of August and for different years to see if the modeled J-values statistics were robust and did not shift. Given the scope of the current work, and the effort from the modeling community, that would not have been possible, and we would have lost participants. As it was, and including some mistakes in diagnostics, the models often had to be corrected and re-run, and the amount of data processed was >60 GB.

The reason for selecting large geographic blocks and 24 hours of model data were to make more robust statistics. Given the limits on available data, we have gone back to the J-values here and sub-sampled our declared "tropical Pacific" region into a west and east half, and also into a narrow stripe down the dateline. This was a useful exercise and the new results are presented for all models in Supplementary figures and discussed in the main text. Basically, most models show no difference across the sub-sampling (NCAR, GFDL, IFS, UCI, UKCA, MOCA) while three models (GC, GMI, GISS) show weaker cloud effects in the East half of the region. This is consistent in that these three use MERRA cloud fields in one way or another.

There was some wish for further analysis of the cloud fields (which would require ice and liquid water paths, effective radii and cloud fraction) and their correlation with J-value anomalies. This new study would be interesting but require much more extensive work from the modelers, and of course, more detailed comparisons of how the models implement the cloud data. This would be better as a model-model set of fixed case studies.

Why not just analyze the cloud fields? or use assimilated/nudged cloud fields?

We chose not to focus on comparing the modeled and observed cloud fields because they really do not tell us how J-values are perturbed by clouds. Moreover, for the observations, there are no observed cloud fields at the resolution of the airplane measurements. J-values vary at the 3-sec resolution of the data (0.8 km) and 3D cloud fields at this scale are not available for the flight from either the aircraft or satellite. There are some marvelous 3D high-resolution cloud fields (on the scale of the aircraft variability), but these are limited to CloudSat-CALIPSO overpasses that have been extended to 200-km wide swaths (see Barker et al., 2011; Miller et al., 2014), not to the 2,000+ km swaths needed to get daily coverage. Even once-a-day coverage will not define clouds over the ATom flight. Assimilating clouds is still a difficult, unsolved problem (from Alan Geer, ECMWF, 2017):

- forecast models still use simplified representations of cloud and convection
- the radiative transfer models required to simulate such 3D structures accurately would be far too expensive for operational use, and
- the predictability of cloud and precipitation tails off in a matter of hours.

A 2018 effort to assimilate clouds in high-resolution models (A.T. White. "Improving Cloud Simulation for Air Quality Studies through Assimilation of Geostationary Satellite Observations in Retrospective Meteorological Modeling", MWR, https://doi.org/10.1175/MWR-D-17-0139.1) is still based on the model physics that creates clouds: "The basic approach is to create positive vertical motion within the model to produce clouds and negative vertical motion to dissipate clouds, based on GOES cloud fields." So we cannot simply use the assimilated or 'nudged' cloud fields. (Nudging uses U, V, T, q not clouds).

An additional reason why we do not spend more time on analyzing the cloud data from the models is that our primary objective is to find out how photochemistry, through J-values, is affected by clouds. The way that models implement clouds can be very different, even when given the same key data: water path and effective radius for ice and liquid, and cloud fraction. In the example pointed out by the reviewers, GC and GMI are both using MERRA clouds and should have similar results: yet, they differ in clear-sky J's; but this difference become greater when we look at all-sky (cloudy) J's. Our analysis here is not a thorough single-test-case model comparison in which one might be able to identify why the models take similar cloud data and use almost the same Fast-J code to give different cloud effects. That would be interesting, but is beyond the scope of this paper.

Barker, H. W., M. P. Jerg, T. Wehr, S. Kato, D. P. Donovan, and R. J. Hogan, 2011: A 3D cloud-construction algorithm for the EarthCARE satellite mission. Quart. J. Roy. Meteor. Soc., 137, 1042–1058, doi:10.1002/qj.824.

Miller, S.D., J.M. Forsythe, P.T. Partain, J.M. Haynes, R.L. Bankert, M. Sengupta, C. Mitrescu, J.D. Hawkins, and T.H. Vonder Haar (2014) Estimating three-dimensional cloud structure via statistically blended satellite observations. J. Appl. Meteor. Climatol., 53, 437–455, doi:10.1175/JAMC-D-13-070.1

Summary. Given that this paper is a start at analyzing how clouds control the statistical variation of J-values, it cannot answer all the questions we have. The reviewers have come up with an interesting set of follow-on questions, which we would all like to see answered. We believe that that we have presented a thorough, innovative approach for assessing how models implement clouds in their photochemistry, and come up with a new type of observational dataset to test this. Some large questions remain as noted in the summary discussion (Section 5). We believe the current content is extensive but necessary to understand this work. Let this be the first step.

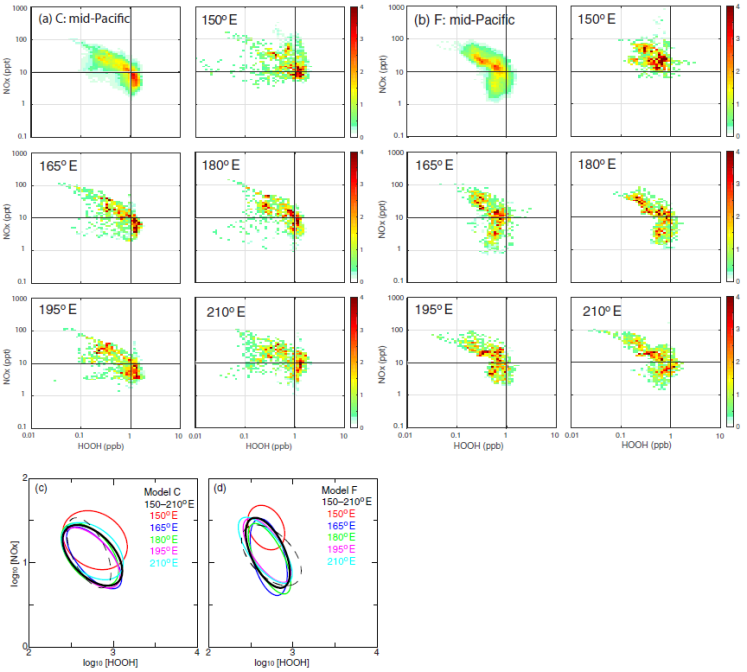

Figure 8. AIR-weighted 2-D probability distributions for NO_y vs. HOOH averaged over tropical Pacific block (150–210° E, 20° S–20° N, 0–12 km) and for different single-longitude transects from 150–210° E, shown for models **(a)** C (GFDL-AM3) and **(b)** F (UCI-CTM). The fitted 2-D ellipses are shown for the full block (thick black line) and five longitude transects (colored lines) for models **(c)** C and **(d)** F. The block ellipse for the other model is shown as a thin black dashed line.

Anonymous Referee #3
Received and published: 14 October 2018

This paper describes the novel use of observation-based photolysis rates derived from aircraft profile flux measurements to test global atmospheric chemistry models. It adopts an original and innovative approach, and provides a highly valuable first step in the evaluation of cloud impacts on photolysis rates in models, deriving some useful pointers to areas that need further exploration or model development. The study is well executed and thorough, exploring sensitivity to ozone column and albedo as well as to a central focus on cloud properties. The analysis approaches appear sound, the conclusions are useful, and as such the paper merits publication in ACP once some minor issues have been addressed.

Thank you.

Specific comments

Data was provided from the models for a single day in August. How dependent are the model results on the specific day chosen? Are the regions large enough to provide a truly representative distribution of cloud coverage? This would be relatively simple to check.

This is a tough question. Please see big-topic answers at the beginning of this response. In part answer your question, we redid the sampling in the tropical Pacific to test the statistics (new Figure S7).

In addition, the number of observed samples per block is stated on page 5, but not the number of low-SZA model samples.

Yes, done. Some numbers were added in text, others in the figure caption.

The coarse resolution of the models leads to an averaging of cloud cover and an under-estimation of clear sky conditions (explored in section 4.3). What would the distribution of rlnJ look like for the observations if these were averaged to the physical scale of the models?

Interesting question. Using data and analyses similar to that for Figure 6, we looked at what happened as we took cloud data from a 640x320 (1/2 degree) model and averaged it over320x160 and 160x80. There was a detectable shift to less-clear skies, but the much bigger effect was on how the cloud fractions are used (Fig. 6). Thus, we deemed it not critical for this paper.

The second part of your question appears to ask about averaging the ATom-1 J's to a 100-km grid. There is no natural registration for such a grid and we did not try it. This would be better when we have added the last 3 deployments and have a larger data set. This topic is very important for model development: the best we can hope for is that modeled J's on 10-100 km scales are effectively the average of the 3D high-resolution fields (i.e., the ATom J's). This is discussed in Section 5.

To what extent does the noise inherent in the observation-based rlnJ values (evident in the broadening seen in Fig 4) wash out the vertical profile of cloud impacts on photolyis rates that is clearly seen in the models?

A very good, but difficult question to answer at this stage. This paper is based on the first released J-cloudy/J-clear ATom-1 data, and it points to the need for further work on

tightening up the spread (noise) in the distribution that could be due to correctable physical processes such as ocean surface albedo, airplane maneuvers (banking and ascent/descent can change the orientation of the 2-pi detectors relative to the direct beam of the sun), etc. When all 4 deployments are available, we can revisit this along with developing an improved set of model diagnostics.

Does the occasional enhancement of near-surface J-values and reduction at high altitudes reflect biases in model cloud distributions, 3-D effects, or just noise?

The low level enhancements are likely due to thinnish clouds where the J's are enhanced within and below. The low-level enhancement in observed J-O1D Tr.Pac. is just not sensible in terms of the 1D modeling, and this is now noted. We need to develop statistics on 3D cloud effects at the scale seen by the aircraft to truly answer this question.

Is Fig 2 based on additional model runs without clouds (alluded to on page 4, line 23) or on clear-sky columns that are a subset of the all-sky data shown in Fig 1? This should be stated on page 6. If the clear-sky values are a subset, what bias does the different locations and SZAs of clear and cloudy columns introduce?

Sorry for the confusion, this is rewritten on page 4 to be explicit: The models submitted two full 24-hour simulations: one with their standard cloud treatment and one where the aerosols and clouds were zeroed. No subsetting.

Fig 5 is an interesting and well thought out way of presenting the data, but is difficult for the reader to interpret, particularly where the bar indicating the proportion of reduced/enhanced J-values does not align with the cross indicating the mean magnitude.

Yes, Fig 5 is a dense figure in terms of information, yet all that information needs to be put together to understand the J statistics. We have added an explanatory legend to Figure 5b (it has the smaller figure caption) and explained more in the text about the 5 values being plotted for each model and the CAFS data.

Minor issues and Typos

Abstract, line 30: "more importantly" Please rephrase this or reorder the sentence appropriately.

Yes, done. Abstract is substantially rewritten in response to reviews.

Page 9, line 25: 3/2 should be a power

Yes, done.

Page 10, line 23: section 4.3 is important, but the title of the section is awkward, please consider rephrasing "finding clear sky".

Yes, done. Thanks."4.3 Averaging over clouds affects clear-sky fraction"

Page 11, line 6-7: this partly repeats information provided on page 5.

Yes, had dropped references and shortened a bit on page 11.

The caption to Figure 6 is too long. The information is valuable, but some of it should be included in the text on page 11. (Typo: please replace star with multiplication sign for consistency)

Agreed. Cut caption, added some discussion to text.

Caption to Fig S2, one line from bottom: "in the in the"

Yes, done.

Caption to Fig S6, line 2: remove second occurrence of "blocks"

Fig S6 needs to be cleaned up so that the titling is legible and the model legend is not superimposed on the axis labels.

Yes, both done.

Anonymous Referee #2
Received and published: 19 October 2018

This paper presented a statistical analysis of the photolysis rates data obtained over the Pacific during the first deployment of the ATom mission (July 29-Aug.6, 2016) and evaluated the performance of nine global models with respect to how clouds affect photolysis rates (J-values). The ATom J-values are a unique data set for testing how well clouds are treated in terms of their impact on photochemistry in current global models. The model J-values presented in this study are from simulations with each model's own configuration without controlling input conditions among all nine models. Comparisons of the probability distributions of cloud impacts on J-values between the models and measurements provided original insights into model performance differences. The paper concludes with an interesting discussion on the difficulties and challenges involved in simulating cloud impacts on J-values and comparing with measurements. The need for more effort to characterize the main factors contributing to the model differences are also acknowledged and discussed. The paper is overall well written and I recommend publication on ACP after some minor modifications.

Thank you.

Title: The title would suggest this paper is about the analysis of photolysis rates from all ATom campaigns, but in fact only the data from ATom-1 (July 29-Aug.6, 2016) is used to test nine global models. The title should reflect these.
Also "climatology" (a term used throughout the text) cannot be derived from a single deployment. "Statistics" is probably a more appropriate term as part of the title for the kind of analysis presented, and is often used in the text.

See overview discussion on these 'big topics'. We now use 'statistics' more and 'climatology' less, but we still have the objective of developing a climatology for all models. Thus the title was changed to indicate the intent to build a climatology. It was impossible to put in all the information about the deployment in the title, and so we put it in the abstract and the opening sections.

Also the published data set (full ATom-1) and the analysis here are clearly stated in the abstract and intro.: "This analysis is limited to the first half of the deployment over the Pacific Ocean, but publishes the complete data set."

Abstract: The abstract could be improved: 1). it doesn't flow that well.

A substantial rewrite was done. Yes, it needed one.

2). P1, L28: "during the first deployment (ATom-1) in August 2016": it's actually July 29-August 6, 2016.

Yes, corrected. The ATom-1 deployment (in air) was 29 Jul to 23 Aug. The data from the tropical Pacific was taken between 29 Jul and 8 Aug (sorry for the 6 Aug typo in the manuscript). This is now accurately described in the paper. The model data is global and the ATom-1 CAFS data archived with this paper are complete, all 10 research flights, 29 Jul – 23 Aug 2016.

3). P1, L29: it would be useful to the reader to state that models provided hourly J-values for a single day of August for the domains measured in ATom-1.

Done. The model data provided here and archived under the doi is one-day global (for 24 hours). Sorry for the confusion.

4). L30: what is the statistical picture of the impact of clouds on J-values established by the ATom-1 measurements?

5). L31-32: "the models show largely disparate patterns", "there is some limited, broad agreement": what are the disparate patterns and broad agreement, specifically?

This section has been revised to give more information, but there remains no single zinging result.

P4, L18: in Table 1

Done, thanks.

P5, L14-16: "It was not possible to have all the models simulate the flight paths and times" - why? Do most of these models use either assimilated or nudged meteorology? "we are trying to develop a climatology" - do you mean "statistics"? "the models were asked to pick a single day in August as representative of the cloud statistics over the large geographic blocks" - A single day of August 1-31, 2016, or near the end of the deployment (prior to Aug.6)? Figure S6 caption mentioned "one day in mid-August". Indicating the selected dates in the "Cloud data" column of Table 1 would help the readers who may want to reproduce or compare the results.

See the Big-Topics overview above. All the models could not do the same year for this project. We now include the Year-Month-Day in Table 1 as requested.

P6, 2nd paragraph: It's worth mentioning and explaining why the GC and GMI models, both driven by the MERRA-2 reanalysis, show large differences in JO1D over the tropical Pacific (upper left panels, Figs. 1-2).

This is now noted in the paper, but the cause is not clear: tropical ozone columns are similar; perhaps different Fast-J datasets?

P9, L11: the sharp peaks P9, L25: superscript "3/2"

Yes, done.

P13, L9, L14: "an observed climatology", "this CAFS climatology" - see above about "climatology".

Yes, this has been cleaned up, see overview.

P20, Table 1: GC "Cloud data" - the model uses liquid and ice cloud optical depths (not liquid and ice water) taken from MERRA-2. GC "Model references" - Gelaro et al. (2017) is the reference for MERRA-2. Cite Liu et al. (JGR 2006, 2009) for GC J-values and B-averaging.

Done.

P20, Table 1: 4th column, GFDL and GMI - what does C1 mean here? GMI "Cloud data" - the model uses liquid and ice cloud optical depths (not liquid and ice water) taken from MERRA-2.

C1 refers to the cloud droplet size distribution (Deirmendjian, 1969) as used in Fast-J. And the table now notes this.

Fig. S1 caption: low SZAs, not high SZAs Fig. S2 caption: "in the in the"

Yes, done, thanks.

Fig. S6 caption: Averaged in-cell cloud optical depth (COD, at 500-600 nm and .....); "blocks studies here blocks".

Yes, fixed. Thanks.

W.J. Collins (Referee)
Received and published: 17 October 2018

Review of Hall et al. 2018
This paper nicely describes J-value measurements as part of the Atom-1 campaign. These measurements and those from further Atom campaigns will provide an excellent resource for assessing chemistry models.

Thanks.

The overall conclusion seems to be that "A primary uncertainty remains in the role of clouds in chemistry. . .". There should be enough information available to the authors to make some more conclusive statements. The authors need to think more about what are the key messages they want people to take away from reading this paper.

Correct. See overview discussion. We have strengthened the last section and made the abstract clearer with some of the results. The problem remains that the comparison we seek is difficult, our results include some clear successes and other places where more work is needed. For example, the observed cloud-reduction in J-values in the uppermost troposphere are not reproduced by the physics of any of the models. We need to look carefully at those data and the flight conditions under which they were made, as well the TUV modeling of the clear-sky conditions. This shift in rlnJ is -0.05, or about 5%.

The paper does not appear very clear as to its main purpose. Model-measurement comparisons can be used to assess whether models are fit for purpose (which doesn't seem the aim here) or to investigate where the models can be improved. This paper touches on the latter, suggesting that there are deficiencies in the treatment of clouds, but not what. It could be that models have too much or too little cloud, or that the frequency pdf of cloud amount is wrong, or that the radiation codes don't treat overlaps correctly or the parameterisation of cloud scattering is wrong. From this paper we still have no idea where to start looking to improve the models. Given the very different results between the observations and (some of) the models it must be possible to give some more concrete statements.

See discussion above. We have taken on the whole picture of the specific questions you list here because the real world consolidates all these. There are many 'degrees of freedom' in these calculations and most of us have done many PhotoComp-like comparisons to address individual model differences. This is the first attempt to diagnose these differences under realistic, climatologically varying conditions. Even the cloud conditions have large uncertainty and cannot simply be fixed for the models from observations. We could declare a full set of cloud data (cloud fraction on a grid cell, ice/liquid effective radius and water path) from some model, but implementing that data in the other 3D models would be painstaking, ranging from using the physics to get optical depth to simply re-gridding. Nevertheless we have added text to clarify the discrepancies between the models and data to elucidate areas for additional study.

A very serious deficiency of the paper is the lack of coincident cloud observations. Cloudy/clear ratios are presented but with no data on what amounts of cloud caused these, it is therefore impossible to know whether the model-measurement differences are caused purely by different clouds. Measurements over 4 days in one particular August cannot be considered a representative

climatology. Were these 4 days more or less cloudy than the climatological average? Where would the observed clouds for these 4 days lie on figure S6? Even if clouds weren't specifically measured by the Atom-1, cloud data will be available from satellite measurements or re-analysis data. This will require a significant amount of work by the authors, but I don't see the value of the paper without this.

The authors respectfully disagree and refer to the discussion above regarding cloud observations. Coincident cloud observations would require 3D lidars, and then modeling would have to use 3D radiative transfer. The authors think this work has value and is the essential first step in evaluating photolysis and photochemistry in a realistic atmosphere. Adding a cloud-field analysis is beyond the scope of this paper but would be an important next step

A significant improvement to the paper would come from plotting the cloudy/clear ratios as a function of cloud fraction (at different levels) for both the models and observations (or reanalysis) – or the authors may come up with a better way of controlling for cloud amount. This would overcome a lot of the issue of likely very different clouds amounts in the 4 particular observed August days with 1 random modelled August day. It would identify whether for the same cloud amount, models and measurements were calculating very different J-values.

See above. Not sure what you mean by 'cloud amount'; every model has a different definition of that. We did not ask the contributors to archive all of their cloud data because the data would not be commensurate. Also it might have caused some participants to drop out, thus limiting the comparison.

Abstract: This needs to contain the key messages from the study.

Agreed. Done.

Page 1: This page seems mostly trying to justify why it is not sensible to do point comparisons. While the real world is 3D, the model radiation codes are typically 1D and so comparing the 1D models with 3D observations would actually seem a sensible test of whether 1D models can represent the real world. More importantly, the claim that 4 days of measurements can be considered a climatology representative even of August 2016 let alone Augusts in general is never questioned. No evidence is presented as to how representative the observed statistics of clear/cloudy might be.

See discussion above. We agree and have withdrawn the 'representative climatology' statements and have added a test of model 'representativeness' with a new figure and discussion of sub-sampling of the Pacific block. Clearly we cannot state how representative the ATom-1 data are at this time. However, we will have the opportunity after adding the data from the last 3 deployments, which should be available early next year.

Page 2, line 8: ". . . net probabilistic distribution of observed J-values". Again this glosses over the issue that the pdfs might be specific to those particular 4 days in August 2016, rather than being a more general climatological probabilistic distribution.

Page 3. Yes, just use 'statistics' – it is really the same thing.

Page 5, line 16: Just as 4 days of observations can't be considered a climatology, a single day in August can't be representative. It should be possible to get much more than a single day's data from these models. Most of the models seem either to use re-analysis or were nudged; did they use meteorological fields from the days of the campaign or a random August?

The models used various meteorological data that were noted in Table 1. The years are varied. Not everyone was able to use 2016 when we collected the data and we did not want to delay the analysis. Now we have added the year-month-day information to that table.

Page 7, line 19: Are the narrow peaks due to the frequency of clouds? It could be that some models have an average cloud fraction of 0.1 by having a fraction of 0.1 every- where, but others have the same mean fraction with a large variety of cloud amounts. PDFs of CF and/or COD are needed (along the lines of fig 6).

The narrow peaks mean simply that for 40% of the time or more, these models have J-values that are within ±2.5% of clear sky – see Figure 5. The cause could be manifold: very thin OD, method of cloud overlap, and even coding errors. CF does not matter unless COD is large enough. For the B-averaging codes, it is $CF^{3/2}xOD$. Comparing details of the cloud data is essential for a single fixed-case photocomp study, but would not clarify the model differences here.

Section 3.2: Given the large differences between the models it is essential to use more than the averaged cloud properties to understand the correlations between CF, COD and J-values, and how these differ between the models. How is COD calculated – does it use the same radiation scheme as for J-values or is from the climate radiation scheme?

See discussion above. The correlations would require an immense new dataset and still not answer some of these questions. A model-model study on clouds and how to implement them would be best addressed by the CCM community.

Section 4.3: It would be useful to use UCI to replicate figure 4 for the ICAs and QCAs to determine how much the averaging contributes to the different distributions in observations and models.

Not sure what this comment is about. UCI standard model runs with QCAs generating a single J-value and a second model version with Briegleb averaging is included (UCIb). To extract the J-values from the individual ICAs is prohibitive since it would increase the cost of the UCI simulation 100x or more. Further, it would require a code re-write to extract sub-resolved J's (ICAs or QCAs) from within the parallelization. The Cloud-J paper (2015) did this with a single fixed-case study.

Conclusions: This paper needs a conclusion section. As it stands it is not at all obvious what the overall conclusion of the study is, other than clouds are difficult and more work is needed.

Conclusions have been updated and are more focused, but an important conclusion remains that which is reflected in your last clause. This paper provides a new statistical analysis to study the effect of clouds on photolysis and hence photochemistry. The limitations of this study are noted, yet the analysis already highlights new aspects (or problems) of the models and differences in modeling techniques.

Cloud impacts on photochemistry: building a ~~new~~ climatology of photolysis rates from the Atmospheric Tomography mission

Samuel R. Hall[1], Kirk Ullmann[1], Michael J. Prather[2], Clare M. Flynn[2], Lee T. Murray[3], Arlene M. Fiore[4,5], Gustavo Correa[4], Sarah A. Strode[6,7], Stephen D. Steenrod[6,7], Jean-Francois Lamarque[1], ~~Jonathon~~Jonathan Guth[8], Béatrice Josse[8], Johannes Flemming[9], Vincent Huijnen[10], N. Luke Abraham[11,12], Alex T. Archibald[11,12]

[1] Atmospheric Chemistry~~,~~ Observations and Modeling Laboratory, National Center for Atmospheric Research, Boulder, CO 80301, USA
[2] Department of Earth System Science, University of California, Irvine, CA, USA
[3] Department of Earth and Environmental Sciences, University of Rochester, Rochester, NY, USA
[4] Department of Earth and Environmental Sciences, Columbia University, NY, NY, USA
[5] Lamont-Doherty Earth Observatory of Columbia University, Palisades, NY, USA
[6] NASA Goddard Space Flight Center, Greenbelt, MD, USA
[7] Universities Space Research Association (USRA), GESTAR, Columbia, MD, USA
[8] Centre National de Recherches Météorologiques, CNRS-Météo-France, UMR 3589, Toulouse, France
[9] European Centre for Medium-Range Weather Forecasts, Reading, UK
[10] Royal Netherlands Meteorological Institute, De Bilt, the Netherlands
[11] Department of Chemistry, University of Cambridge, Cambridge, U.K.
[12] National Centre for Atmospheric Science, U.K.

Correspondence to: Michael J. Prather (mprather@uci.edu)

Abstract. Measurements from actinic flux spectroradiometers on board the NASA DC-8 during the Atmospheric Tomography (ATom) mission provide an extensive set of statistics on how clouds alter photolysis rates (J-values) throughout the remote Pacific and Atlantic Ocean basins. ~~ATom made profiling circumnavigations of the troposphere over four seasons during 2016-2018.~~ J-values ~~are a primary chemical~~ control ~~over~~ tropospheric ozone and methane abundances, and ~~their greenhouse effects. Clouds~~thus clouds have been ~~recognized~~included for more than three decades ~~as being an important factor~~ in tropospheric chemistry~~. The ATom climatology~~ modeling. ATom made four profiling circumnavigations of the troposphere capturing each of ~~J-values is a unique test of how~~ the ~~chemistry models treat clouds.~~ seasons during 2016-2018. This work ~~focuses on measurements over~~examines J-values from the Pacific ~~during~~ Ocean flights of the first deployment ~~(ATom-1) in~~, but publishes the complete Atom-1 data set (29 July to 23 August 2016~~. Nine~~). We compare the observed J-values (every 3 sec along flight track) with those calculated by nine global chemistry–climate ~~or~~ /transport models ~~provide J-values~~ (globally gridded, hourly, for ~~the domains measured in ATom-1. We compare mean profiles over a range of cloudy and clear conditions; but, more importantly~~a mid-August day). To compare these disparate data sets, we build a commensurate statistical picture of the impact of clouds on J-values ~~through the distribution of~~ using the ratio of J-cloudy (standard, sometimes cloudy conditions) to J-clear~~. In detail,~~ (artificially cleared of clouds). The range of modeled cloud effects is inconsistently large but fall into two distinct classes: (1) models with large cloud effects showing mostly enhanced J-values aloft and or diminished at the surface; and (2)

models ~~show largely disparate patterns. When compared with measurements, there is some limited, broad agreement. Models~~with small effects having nearly clear-sky J-values much of the time. The ATom-1 measurements generally favour large cloud effects but are not precise or robust enough to point out the best cloud-modeling approach. The models here have resolutions of 50-200 km and thus reduce the occurrence of clear sky when averaging over grid cells. In situ measurements also average ~~the~~ scattered sunlight over a mixed cloud field, but only out to scales of 10s of km. A primary uncertainty remains in the role of clouds in chemistry, in particular, how models average over cloud fields, and how such averages can simulate measurements.

1 Introduction

Clouds visibly redistribute sunlight within the atmosphere, thus altering the photolytic rates that drive atmospheric chemistry (J-values), as well as the photosynthesis rates on the land and in the ocean. These J-values drive the destruction of air pollutants and short-lived greenhouse gases. The NASA Atmospheric Tomography Mission (ATom, 2017; Wofsy et al., 2018), in its charge to measure the chemical reactivity over the remote ocean basins, has measured J-values while profiling the troposphere (0 – 12 km). These measurements reveal a statistical pattern of J-values over different geographic, altitude and cloud regimes, which directly challenges current atmospheric chemistry models and provides a new standard test of cloud effects. The observations quantify how clouds alter photochemistry and are compared here with parallel analyses from nine global atmospheric chemistry models.

Since the early models of atmospheric chemistry, the scientific community has tried various approximations and fixes for "those pesky clouds". Overhead clouds can shadow the sun, resulting in ~~reduced~~diminished J-values beneath and within the lower parts of thick clouds. Cloud scattering results in enhanced J-values above and within the tops of clouds. For ideal clouds – uniform layers from horizon to horizon – the models have developed a variety of methods to approximate the 1D radiative transfer and calculate the J-values relative to a clear sky (Logan et al., 1981; Chang et al., 1987; Madronich, 1987; Wild et al., 2000; Lefer et al., 2003; Williams et al., 2006; Palancar et al., 2011; Ryu et al., 2017). More realistic treatment of clouds is important in global chemistry as well as air pollution (Kim et al., 2015). For the most part, these chemistry models are provided with the cloud properties and fractional coverage for each grid cell in a column, ~~and then~~ make some assumptions about the overlap of cloud layers, and then solve the 1D plane-parallel radiative transfer equation at varying levels of accuracy. In a 3D world, however, adjacent clouds can block the sun or scatter light even when there are clear skies overhead. Also in a 3D world, a sunlit adjacent cloud that is not overhead can increase J-values. It is nigh impossible to specify the 3D cloud fields at ~1 km scale along the ATom flight paths or any similar mission~~; and, further~~: 3D high-resolution cloud fields on this are available, but these are limited to CloudSat-CALIPSO afternoon overpasses extended to 200-km wide swaths (see Barker et al., 2011; Miller et al., 2014). Anyway, none of the standard global models can deal with such a 3D radiative transfer problem. So accepting the model limitations and the inability to match individual measurements, we use the ~~observed~~ statistics

of observed J-~~value increases/decreases~~values, enhanced or diminished relative to a clear sky, and ask if the models' many approximations for the radiative transfer in cloud fields can yield those same net results.

This paper presents the statistical distribution of the measured J-values using the CAFS instrument (Charged-coupled device Actinic Flux Spectroradiometers: Shetter and Mueller, 1999; Petropavlovskikh et al., 2007) from the first ATom deployment ~~in~~(29 July through 23 August 2016~~. Specifically, we look at~~). We build up statistics of the observed J-value relative to that calculated for a clear sky under similar conditions. The chemical reactivity of the troposphere (see Prather et al., 2017) is generally proportional to these changes in J-values, and thus modeling of the variability of clouds is critical for modeling the lifetime of CH_4 and the cycling of tropospheric O_3.

So what makes this model versus measurement comparison different? The atmospheric chemistry community has a history of such comparisons, including photolysis rates, dating to the early ozone depletion assessments (Nack and Green, 1974; M&M, 1993) and continuing to recent multi-model projects (Olson et al., 1997; Crawford et al. 2003; PhotoComp, 2010). These comparisons have been limited mostly to simplistic atmospheric conditions and measurements made under clear skies or with uniform 1D cloud layers for which an accurate solution can usually be calculated. We introduce here the ability to use CAFS all-sky measurements made under a semi-objective sampling strategy (i.e., ATom's tomographic profiling makes pre-planned slices through the troposphere, limited by available airports, diverting only for dangerous weather). We test the collective treatment of clouds and radiation in models insofar as they can match the ~~net probabilistic distribution of~~ observed statistics of J-values. This approach gets to the core of atmospheric photochemistry by combining the range of assumptions and parameterizations for clouds in the models including, among others, cloud optical depths and scattering phase functions, two-stream or multi-stream radiative transfer, cloud overlap, or even just parametric correction factors.

Section 2 describes the measurements and models, including how the observational statistics are compiled, what protocol the models used, and how they included cloud fields. This section also documents the differences in mean J-values, which can be as large as 30% in either cloudy or clear conditions. Section 3 introduces the statistical distributions based on the ratio of full-sky including clouds to clear-sky. Section 4 examines modeling errors and improvements related to this comparison. In the concluding Section 5, we discuss the current range in modeling cloud effects and how new observational constraints can be developed and used to build better models.

2 Measuring and Modeling J-values under Realistic Cloudy Skies

Here, we focus on two J-values: $O_3 + hv \rightarrow O_2 + O(^1D)$ designated J-O1D; and $NO_2 + hv \rightarrow NO + O(^3P)$ designated J-NO2. These J-values are the most important in driving the reactive chemistry of the lower atmosphere, and each emphasizes a different wavelength region with response to atmospheric conditions. J-O1D is driven by short wavelengths (<320 nm), where

O_3 absorption and Rayleigh scattering control the radiation; whereas J-NO2 is generated by longer wavelengths, where O_3 absorption is not important and Rayleigh scattering is 2 times smaller. Thus, J-NO2 is the more sensitive J to clouds. Both CAFS and the models accept the same spectral data – cross sections and quantum yields from recent assessments (Atkinson et al., 2004; Burkholder et al., 2015) – but the implementation (solar spectrum, Rayleigh scattering, wavelength integration, temperature interpolation) may be different.

Spectrally resolved CAFS measurements of actinic flux (280-650 nm) are used to calculate in situ J-O1D and J-NO2. These observed J-values are all-sky J-values and include incidences when the sky is effectively clear of clouds. We designate these all-sky J-values as J-cloudy in both measurements and models to contrast them with the artificially cloud-cleared J-values denoted J-clear. For J-clear, CAFS uses the Tropospheric Ultraviolet and Visible (TUV) radiative transfer model (Madronich and Flocke, 1999). The model is run with an eight-stream discrete ordinate radiative transfer method with a pseudo-spherical modification to generate actinic fluxes with a 1-nm wavelength grid from 292-700 nm. The calculation is run with no clouds and no aerosols, a fixed surface albedo of 0.06, and applies ozone columns from the satellite Ozone Monitoring Instrument (Levelt et al., 2006; Veefkind et al., 2006). CAFS and TUV spectra are processed using the same photolysis frequency code to ensure that the same quantum yield, absorption cross section, and temperature and pressure dependence relationships are applied to the measured and modeled spectra. The strong connection between measurement and model has been established in past campaigns (Shetter et al., 2002, Shetter et al., 2003, Hofzumahaus et al., 2004). The ATom CAFS data set used here is a value-added product beyond the standard ATom output (Wofsy et al., 2018), and it is archived with this paper. Only data from the first deployment, ATom-1, were available when this paper was being prepared.

Global chemistry models cannot be used productively in comparisons with individual CAFS observations as noted above, but a statistical comparison of the ratio J-cloudy to J-clear is a useful climatological test. It is difficult for the models to simulate CAFS global data unless there is a very careful sampling strategy to match albedos from the ATom flights over land and cryosphere. Thus, we focus on the 2 oceanic blocks in the Pacific for which we have a large number of measurements with high sun in ATom-1. See also discussion of ocean surface albedo variations in Section 4. The CAFS statistics are derived from the ATom-1 deployment and selected for 2 remote geographic blocks in order to compare with the models: (block 1) Tropical Pacific, 20S-20N x 160E-240E; and (block 2) North Pacific, 20N-50N x 170E-225E.

The models here include the 6 original ones used in the ATom reactivity studies (Prather et al., 2017) plus 3 additional European global chemistry models. They are described more fully in ~~the~~ Table 1, and are briefly designated as: GEOS-Chem (GC); GFDL AM3 (GFDL); GISS Model 2E1 (GISS); GSFC GMI (GMI); ECMWF IFS (IFS); MOCAGE (MOCA); CESM (NCAR); UCI CTM (UCI); and UM-UKCA (UKCA). Additional model information and contacts are given in Supplementary Table S1. All models submitted global 4D fields (latitude by longitude by pressure for 24 hours) for one day in mid-August using their standard treatment of clouds (designated all-sky or "cloudy" here) and then a parallel simulation with clouds and

aerosols removed (designated clear-sky or "clear"). In addition to its correlated cloud-overlap model with multiple quadrature column atmospheres to calculate an average J-value, UCI also contributed a model version using the B-averaging of cloud fractions (Briegleb, 1992) used by most models, designated UCIb (see Prather, 2015). Several models ran the clear-sky case without clouds but with their background aerosols. Globally, aerosols have a notable impact on photolysis and chemistry (Bian et al., 2003; Martin et al., 2003), but over the middle of the Pacific Ocean (this analysis), the UCI model with and without aerosols shows mean differences of order ±½%.

Modeling the effect of clouds on J-values began with early tropospheric chemistry modeling. One approach was to perform a more accurate calculation of generic cloud layers offline and then apply correction factors to the clear-sky J's computed inline: e.g., an increase above the cloud deck and a decrease below (Chang et al., 1987). Another approach used a climatology of overlapping cloud decks to define a set of opaque, fully reflecting surfaces at different levels: e.g., the J's would be averaged over these sub-grid column atmospheres (Logan et al., 1981; Spivakovsky et al., 2000). As 3D tropospheric chemistry models appeared, the need for computationally efficient J-value codes led to some models ignoring clouds and others estimating cloud layers and applying correction factors to clear-sky J's. With the release of Fast-J (Wild et al., 2000), some 3D models started using a J-value code that directly simulated cloud and aerosol scattering properties with few approximations. The next complexity, based on general circulation modeling, included fractional cloud cover within a grid cell and thus partial overlap of clouds in each column (Morcrette and Fouquart, 1986; Briegleb, 1992; Hogan and Illingworth, 2000). This approach later moved on to chemistry models (Feng et al, 2004; Liu et al., 2006; Neu et al., 2007). Monte Carlo solutions for the numerous independent column atmospheres generated by cloud overlap were developed for solar heating (MCICA: Pincus et al., 2003), but random, irreproducible noise was not acceptable in deterministic chemistry-transport models. The Cloud-J approach (Prather, 2015) developed a scale-independent 1D method for cloud overlap based on vertical decorrelation lengths (Barker, 2008a, 2008b). The chemistry models here use a ~~range~~variety of these methods, which range from lookup tables with correction factors, to Fast-J single column, to cloud overlap treatments with Cloud-J, see Table 1. Currently these models do not attempt to define 3D cloud structures within a grid square, the approach needed to match individual CAFS J's.

The CAFS data were collected from ATom-1 during its 10 research flights ~~1-4~~ from 29 Jul to ~~6~~23 Aug 2016. It was not possible ~~to have all~~for the models simulate ~~the~~each flight ~~paths~~path, including clouds and ~~times, and because we are trying to develop a climatology, the~~ local solar zenith angles (SZA) for each measurement. Not all of the models ~~were~~ could run with 2016 meteorology, and thus we asked ~~to pick~~for a ~~single~~ day in mid-August and treat that (rightly or wrongly) as ~~representative~~typical of the cloud statistics ~~over the~~ during ATom-1. The meteorological years are listed in Table 1. This simplification made it possible to attract large ~~geographic blocks~~participation, but of course it limits the ability to claim that the model statistics are a robust climatology. ATom flights are mostly in daylight and hence a large proportion of CAFS measurements occur at high sun, cos(~~Solar Zenith Angle~~SZA) > 0.6, with more than half at cos(SZA) > 0.8 (Supplementary Figure S1). The models report hourly J-O1D and J-NO2 globally over 24 hours, and thus all have a similar distribution of

cos(SZA) but with a greater proportion at cos(SZA) < 0.4 than the CAFS data. We restrict these comparisons to high-sun, cos(SZA) > 0.8, to reduce three-dimensional effects that are not modeled here, which leaves 11,504 (block 1) and 4,867 (block 2) measurements for the CAFS/TUV 3-sec averages. For the models, the number of hourly samples with cos(SZA) > 0.8 is about 18% for both blocks and thus the number of samples depends on model resolution (e.g., 240,000 for UCI and 1,400,000 for NCAR in block 1). Although the analysis here is limited to the Pacific blocks, the global model data are archived with this paper.

A quick look at J-cloudy (all sky) profiles of J-O1D and J-NO2 for CAFS (Figure S2) shows a basic pattern also seen in models. Both J's are larger in the upper troposphere where the direct sunlight is more intense; but in the northern Pacific, larger cloud cover and more scattered light almost reverses this pattern with enhanced J's at lower altitudes (>600 hPa). Comparing the variances of J-cloudy (CAFS) and J-clear (TUV) for the tropical Pacific, the J-NO2 variability is driven almost entirely by clouds as expected, while the J-O1D variability is driven firstly by O_3 column and sun angle (both CAFS and TUV), while there are clearly cloud contributions (CAFS only) at lower altitudes (>700 hPa).

Figure 1 shows a full comparison of the CAFS J profiles with the 10 model results in 4 panels (2 J's x 2 geographic blocks). The CAFS J's fit within the range of models; their shape is matched by most models; but the model spread of order 20-30% is hardly encouraging. Differences in these average profiles can have many causes: temperature and O_3 profiles; spectral data for both J-O1D and J-NO2; ways of integrating over wavelength; surface albedo conditions; treatment of Rayleigh scattering; basic radiative transfer methods; ~~solar zenith angle~~SZA; and, of course, clouds. In typical comparisons we try to control for these differences by specifying as many conditions as possible; but here we want to compare the 'natural' J's used in their full-scale simulations (e.g., Lamarque et al., 2013) and thus leave each model to its native atmospheres, spectral data, algorithms and approximations.

The models show a much tighter match in J profiles under clear-sky conditions (Figure 2). Typically, 8 of the models fall within 10% of their collective mean profile. Some models are obviously different in J-clear (GISS and MOCA for J-O1D, MOCA for J-NO2), and these differences carry through to J-cloudy (Figure 1). A most important factor in J-O1D is the O_3 column, and Figure S3 shows the modeled O_3 columns for August compared with 8 years of OMI observations. MOCA, NCAR and IFS have low tropical O_3 columns, <250 DU vs. observed ~265 DU, which could lead to higher J-O1D, but this effect is seen only in MOCA. UKCA has higher tropical columns, >300 DU, which might explain why their J-O1D lies in the lower range of the models. Some results, like MOCA's J-NO2 and GISS's J-O1D point to differences in the implementation of spectral data (e.g., wavelength integration, solar spectrum, temperature interpolation). We expect GC and GMI to be alike since they both use MERRA-2 cloud fields and Fast-J with Briegleb averaging: indeed, they match well except for J-O1D in the tropical Pacific, yet, they report similar tropical ozone columns.

The ratio of J-cloudy to J-clear, shown in Figure 3, cancels out many of the model differences in Figures 1 and 2, ~~but it~~and as expected GC and GMI are nearly identical. The cloudy:clear ratio identifies new patterns in model differences whereby some models have ratios close to 1 throughout the troposphere (especially in the tropics) while others have ratios >1.1 at altitudes above 800 hPa and <0.9 below 900 hPa. In a recent model intercomparison with specified chemical abundances (Prather et al., 2018), we found that the tropospheric photochemistry of O_3 and CH_4 responded almost linearly to cloudy-clear changes in J-values (see Figure S4, data not shown in Prather et al., 2018). Thus the differing impact of clouds on J-values seen in Figure 3 will have a correspondingly impact on global tropospheric chemistry (see Liu et al., 2009).

3 The Statistical Distribution of J-cloudy to J-clear

The average ratio of J-cloudy to J-clear (Figure 3) provides only a ~~limited~~single measure of the impact of clouds. The CAFS data provide a more acute measure by sampling the range of cloud effects ~~(% increase~~(enhance or ~~decrease~~diminish J-values) and their frequency of occurrence. A quick look at this range in CAFS data is shown in Figure S5 with the probability of occurrence of the cloudy-to-clear ratio defined as ln(J-cloudy/J-clear) and designated rlnJ. Each curve is normalized to unit area with the Y-axis being probability per 0.01 bin (~ 1 %) in rlnJ.

We expect that ~~increases~~enhancements in J's occur above clouds and ~~decreases~~diminishments below, and this is borne out in Figure S5. In the marine boundary layer (900 hPa – surface), there are a greater number of rlnJ < -0.10 with fewer rlnJ > 0.00. In the mid-troposphere layer (300 – 900 hPa), there are frequent occurrences of rlnJ > +0.10 particularly in the North Pacific where lower level clouds are more extensive than in the tropics. Likewise, there are times when rlnJ is < 0.00 in the mid-troposphere when ~~these~~ clouds lie overhead. In upper tropospheric layers (100 – 300 hPa), most of the optically thick clouds are below and rlnJ > 0.00 is dominant. Thus, our analysis here breaks the atmosphere into these 3 layers. All figures in this section will be displayed as 2-block by 3-layer panels with part a (J-O1D) and part b (J-NO2).

3.1 Modeling the distribution of J-values

The probability distribution of rlnJ for J-O1D (Figure 4a) and J-NO2 (Figure 4b) shows highly varied patterns across the models, but with some consistency. The models and CAFS are not exactly a match, but again, there are some encouraging patterns. The peak rlnJ distributions for CAFS will be broadened because the real variation in ocean surface albedo is not simulated in TUV (see discussion in Section 4), but this is expected to be of order ±2%, and so the overall width (10 to 20 %) reflects cloud variability. The modeled and measured distributions are asymmetric and skewed toward rlnJ > 0 in the free troposphere (100 – 900 hPa), and toward rlnJ < 0 in the boundary layer. This pattern is expected since J's are enhanced above clouds (100 – 900 hPa) and ~~reduced~~diminished below. There will also be some occurrences of rlnJ < 0 in the free troposphere when thick clouds are overhead, but none of the models come close to the CAFS frequency of these occurrences. In general and as expected, this brightening above and dimming below is more evident for J-NO2 than for J-O1D. Another feature that

is somewhat consistent across models and observations: the wings of the rlnJ distribution are wider in the North Pacific than the Tropics. In the boundary layer, observations and models show the reverse with greater cloud effects (dimming, rlnJ < 0) in the Tropics. Although all the models show this shift from rlnJ > 0 to rlnJ < 0 in the peak of their distributions, only a few (GISS, MOCA, NCAR, UCI) have broad wings of large cloud shielding (rlnJ < -0.1). These models calculate such broad wings for both Tropics and North Pacific; whereas CAFS only shows this in the Tropics.

These diagnostics also identify some CAFS anomalies that have no physical basis in the current models. For example, low-level (surface to 900 hPa) observed cloud enhancements (rlnJ > 0.025) observed in the tropical Pacific (particularly J-O1D) does not appear in the models. Similarly cloud diminishments in the upper troposphere do not appear with the modeled cirrus. A more thorough analysis of the CAFS rlnJ with the added deployments should examine if these differences are due to 3D radiative transfer effects, ocean albedo variations, or missing cloud types in the models. Perhaps, we will identify sun-cloud geometry conditions simply not possible in the 1D cloud models.

Figures 5a (J-O1D) and 5b (J-NO2) provide another view of the rlnJ statistics. Figure 5 has the same 6 blocks as figure 4, but plots 5 quantities schematically in a single line describing each model's statistics: percent occurrence of diminishment (rlnJ < –0.025), average rlnJ diminishment, percent occurrence of nearly clear sky, percent occurrence of enhancement (rlnJ > +0.025), and average rlnJ enhancement. The horizontal line has total length of 100% with the thin line (clear sky) centered on 0, see the extended legend in Figure 5b.

Overall, four models (GC, GFDL, GMI, UKCA) have unusually narrow peak distributions of rlnJ ~ 0, indicating lesser cloud effects on the J's. The other 6 models (GISS, IFS, MOCA, NCAR, UCI, UCIb) show a much greater range in J's, with a larger fraction perturbed by clouds (~~increased~~enhanced or ~~decreased~~diminished by more than 10%). The CAFS observations generally support this latter group. There are individual model anomalies that may point to unusual features: MOCA alone has a peak frequency of enhanced J's at rlnJ ~ 0.05 in the free troposphere; three models (NCAR, UCI, UCIb) show the largest extended frequency of |rlnJ| > 0.10 in the middle troposphere; UKCA is consistently the most "clear sky" model. These model differences are not simply related to the model cloud fields, see discussion of Figure S6 below.

Immediately above and below extensive thick cloud decks the dimming/brightening of J's exceeds the plotted range of rlnJ of ±0.3 (a factor of 1.35). Most such cloud decks occur around 900 hPa and so the largest brightening occurs in the 100-900 hPa levels, and the greatest dimming at >900 hPa. The top two rows in Figure 4 give the fraction of samples for which rlnJ > 0.3 on the right side of each plot; the bottom row gives, on the left side, the fraction for which rlnJ < -0.3. The categorization of models and measurements is not simple as many models have shifting magnitudes of this large-scale brightening or dimming. A few models consistently lack these large changes in J's (GC, GMI), and a few always have them (NCAR, UCIb). Large CAFS values are clearly evident in both J's for only 2 of the 6 cases: >900 hPa in Tropical Pacific (13 – 15 % of all J's) and

300-900 hPa in North Pacific (8 – 15 %). For these cases the CAFS extreme fractions are consistent with at least 4 of the models. Any possible CAFS bias in rlnJ due to TUV modeling (±0.05) is unlikely to affect these results. These extreme fractions, however, are likely sensitive to any sampling bias of flight path with respect to thick cloud decks, and this needs to be assessed with model sampling that matches the ATom-1 profiles of that period.

The large geographic blocks were chosen to acquire representative sampling from the models that would be repeatable over time. It was not possible to acquire month-long or multi-year diagnostics from all the models, and so with the available model results (24 hours from a day in mid-August) we sub-sample the broad tropical Pacific block (20S-20N x 160E-240E) into a west (160E-200E), east (200E-240E) and dateline (175E-185E) blocks. The results of these sub-sampled statistics are shown for J-NO2 in Figures S7a (100-300 hPa) and 7b (surface-900 hPa) using the same format as Figure 5. Each of the 18 panels in Figure 7ab represents a single model and a single pressure level for which there are 7 bars (sampled distributions of rlnJ). The top 4 bars show the full tropical Pacific (as in Figure 5b) and then the 3 sub-sampled regions. The next 3 bars are the previously sampled statistics (north Pacific, global 50S-50N, and tropical Pacific CAFS). The CAFS bars are the same in each 9-panel plot. Six models show no difference across the sub-sampling (NCAR, GFDL, IFS, UCI, UKCA, MOCA), while three models using MERRA cloud fields in one way or another (GC, GMI, GISS) show weaker cloud effects in the east half of the region. For the most part, the sub-sampled regions have similar statistics that are distinct from the CAFS observations. Thus our model statistics over a large block may be a representative climatology of cloud effects on J-values. Further sampling tests are recommended for follow-on work, especially to determine if the distinct east-west differences for the 3 MERRA-cloud models are a standard feature.

3.2 Analyzing cloud effects

With a graphical synopsis of the rlnJ probability distributions in Figures 5ab, some model features become more obvious. We define nearly cloud-free conditions as being within ±2.5 % of clear-sky J's, and show the frequency of these with the length of the thin line in the center of the plots. Starting with the J-O1D in the upper Tropical Pacific, we find 5 models (Group 1: GC, GFDL, GMI, GISS, UKCA) show no effect of clouds more than 50 % of the time. The other 40 – 50 % of the time, they show enhanced J-O1D, cloud brightening expected from clouds below (thick lines on the right side of the plot). For the other 5 models (Group 2: IFS, MOCA, NCAR, UCI, UCIb), these clear-sky equivalent J's occur only 10-20% of the time, with cloud brightening enhancements occurring at 80 – 90 %. Surprisingly, both model groups show the same average magnitude, +10 % (X's on the right side), for their enhanced J's. Thus Group 2 models will have systematically greater J-O1D in the upper Tropical Pacific than the Group 1 models (i.e., the 10 % enhancement occurs twice as often). In the North Pacific, this pattern holds although both groups show slightly greater frequency of enhanced J's, e.g., 50 to 60 % for Group 1 and 80 to 90 % for Group 2. For J-NO2, the results are similar, but with greater average magnitude of enhancement for cloudy skies (20 % vs. 10 %) and a slightly greater frequency of occurrence (thick line on the right). For this upper tropospheric layer, none of the

models show significant occurrence of ~~dimming~~diminished J-values from overhead clouds (rlnJ < -0.025) as seen in CAFS for 2 – 12 % of the measurements.

In the middle troposphere (300 – 900 hPa, middle panels), the patterns in clear-sky frequency remain unchanged, but there is a shift to cloud dimming for 5 to 20% of the time. This shift to more cloud obscuration is much greater in CAFS than in any model. Group 1 models show consistently more frequent cloud obscuration (10-20%) than do Group 2 models (5-10%). When cloud brightening occurs (both CAFS and models), the magnitude of enhancement is greater than in the upper troposphere. Such a pattern is consistent with the simple physics that J's are greater immediately above a cloud than high above it.

In the boundary layer, most clouds are above, and cloud obscuration leads to increased occurrence of rlnJ < -0.025 compared to the middle troposphere (in both CAFS and models). Even though the frequency changes, the average magnitude of ~~reduction~~diminishment when there is cloud obscuration (denoted by X's) does not change much across models in either region. For CAFS in the Tropical Pacific, however, the ~~reduction~~diminishment when there is cloud obscuration is much larger in the boundary layer. The modeled shifts in frequency of occurrence from enhanced to reduced J's are dramatic, but still the Group 1 pattern of nearly 50% clear-sky J's persists. This results in Group 2 having a much larger frequency of ~~reduced~~diminished J's (60-80%) as compared with Group 1 (20 – 40 %).

Using CAFS data to define nearly cloud-free conditions is imperfect. Potential biases exist with TUV modeling of J-clear and are related to albedo as discussed in Section 4. In addition, the CAFS data does not represent a true climatology due to flight planning and flight operations that tend to avoid strong convective features and thick cloud decks, particularly near the surface. Such biases can shift the distribution as well as widen it through noise, and this may explain some of the increased width of the CAFS peak and the 1 to 2% offsets of the clear-sky peaks in Figures 4. It is difficult to select between Group 1 and 2 using CAFS. The CAFS clear-sky fraction lies between that of the two groups in the upper troposphere but becomes narrower in the boundary layers, more closely matching that of Group 2. Given that a number of processes can lead to broadening of the CAFS distribution, it is likely ~~that~~ the sharps peaks in Figure 4 (and wide central lines in Figure 5) of Group 1 are unrealistic.

These model differences have no obvious, single cause. The modeled profiles of cloud optical depth (COD) and cloud fraction (CF) for both geographic blocks are shown in Figure S6 (note the logarithmic scale for COD). The total COD is given (color-coded) in each block. The profiles show very large variability that is hard to understand. For example, GFDL and GISS show the largest COD, yet both are in Group 1 with the largest fraction of clear sky. Overall the total COD does not obviously correlate with the two groups. Likewise, CF is not a predictor for the Group. It is likely that model differences are driven by the treatment of fractional cloud cover. For example, GMI (Group 1) and UCI (Group 2) have very similar cloud optical depths (COD) and cloud fractions (CF) in the lower troposphere as shown in Figure S6. They also use similar J-value codes including spectral and scattering data based on the Fast-J module. Yet, they have a factor of 2 difference in the frequency of

nearly cloud-free sky as shown in Figure 5. Compared to GMI, UCI shows an overall greater impact of clouds with 2x larger frequency of cloud brightening in the upper troposphere and 2x larger occurrence of cloud dimming in the boundary layer. These differences could be caused by GMI calculating J-values with a single column atmosphere (SCA) containing clouds with Briegleb ($CF^{3/2}$~~)~~) averaging and UCI calculating J-values with four quadrature column atmospheres (QCAs), see Table 1. Unfortunately, when UCI mimics the B-averaging (with model UCIb), the differences remain. See further discussion of Figure S6 in Section 4.1.

4 Model Difficulties and Development

The J-value statistics here depend on (i) the cloud fields used in the models, (ii) the treatment of cloud overlap statistics, (iii) the radiative transfer methods used, and (iv) the spectral data on sunlight and molecular cross sections. These components are deeply interwoven in each model, and it is nearly impossible to have the models adopt different components except for (iv), where there has been a long-standing effort at standardization (e.g., the regular IUPAC and JPL reviews of chemical kinetics, Atkinson et al., 2004; Burkholder et al., 2015). These components are briefly noted in Table 1.

4.1 Cloud optical depths and overlap statistics

The models reported their average in-cell cloud optical depth (per 100 hPa) and cloud fraction over the two Pacific blocks in Figure S6. Averaged cloud optical depths (defined for the visible region 500-600 nm) all tend to peak below 850 hPa in the tropics and decline with altitude. There is clear evidence of mid-level (400-800 hPa) clouds, but only small COD (total < 0.25) at cruise altitudes (100-300 hPa). The North Pacific block has 2-4x larger low-altitude COD. The plotted cloud fraction (CF) is the COD-weighted average over 24 hours and all grid cells in the block. Note that for COD the cloud is spread over each model layer, and hence the in-cloud optical depth is estimated by COD/CF. CF is high, 5-15% below 850 hPa, drops off with altitude as does COD, but peaks at 10-20% near 200 hPa corresponding to large-scale cirrus. Some of these differences in COD and CF are large enough to explain model differences; but there is no clear pattern between J-values and clouds as noted in Section 3.2. A more thorough analysis and comparison of the modeled cloud structures would involve the full climate models and satellite data (Li et al., 2015; Tsushima et al. 2017; Williams and Bodas-Salcedo, 2017), beyond the scope here.

4.2 Sensitivity of rlnJ to small cloud optical depth

To relate total COD to a shift in rlnJ, the UCI offline photolysis module Cloud-J was run for marine stratus (CF = 1) with a range of total CODs from 0.01 to 100. The cloud was located at about 900 hPa and rlnJ evaluated at 300 hPa. The plot of rlnJ vs log COD for a range of SZA is shown in Figure ~~S7~~S8. A 10 % enhancement (rlnJ = +0.10) occurs at COD = 5 for J-O1D and COD = 3 for J-NO2, demonstrating the greater sensitivity of J-NO2 to clouds. Thus model average total COD (ranging from 0.8 to 11 in Figure S6, assuming CF=1) should produce large shifts in rlnJ. Marine stratus with typical COD ~10 or more would produce rlnJ-O1D of +0.16 and rlnJ-NO2 of +0.30. Thus clear-sky J-values (defined here as ±0.025 in rlnJ) require

COD < 1 for J-O1D and < 0.3 for J-NO2. A COD ~ 1 is not that large since these clouds are highly forward scattering and have an isotropic-equivalent optical depth that is 5x smaller.

4.3 Averaging over clouds ~~and finding~~affects clear ~~-~~sky fraction

Comparison of the CAFS-ATom measurements of J-values with modeled ones presents a fundamental disconnect, but one that we must work through if we are to test the J-values in our chemistry-climate models with measurements. A CAFS observation represents a single point with unique solar zenith and azimuth angles within a unique 3D distribution of clouds and surface albedos. Ozone column and temperature also control J-values but are less discontinuous across flight path and model grids. One can define a column atmosphere (CA) for each J-value in terms of the clouds directly above/below and the surface albedo, as would be measured by satellite nadir observations. The CAFS measured actinic flux includes direct and diffuse light, which depends on all the neighboring ~~CAFS~~CAs out to 10s of km. Adjacent clouds can either increase or decrease the scattered sunlight at the measurement site depending on location of the sun.

By including cloud fractional coverage from the meteorological models, and attempting in various ways to describe cloud overlap, the models here recognize that the atmosphere is not horizontally homogeneous. Yet, for cost effectiveness and non-random J-values, most modeling solves the ~~RT~~radiative transfer problem for a 1D plane-parallel atmosphere that is horizontally homogeneous. Most chemistry models adopt a simple averaging procedure to create a single, horizontally homogeneous cloudy atmosphere in each grid cell and then solving for a single J-value (see Table 1). The UCI model uses ~~a combination of maximum overlap and~~ decorrelation lengths ~~(Barker, 2008a, 2008b; Prather, 2015)~~to determine cloud overlap, to generate ~~an ensemble~~a set of independent column atmospheres (ICAs), to generate 4 quadrature column atmospheres (QCAs), to calculate 4 J-values, which are then averaged to get a single J-value. In either case, the ~~RT~~radiative transfer solution is 1D and there is one J-value per grid cell given to the chemistry module (and analyzed here).

What would the probability distribution rlnJ look like if we used the UCI J-values from the QCAs before averaging? For this, we collect the statistics on total COD for the two geographic blocks and compare the sub-grid QCA CODs against averaging approaches in Figure 6. ~~The QCA distribution is very close to the full ICA distribution (see Prather, 2015). If the cloud fields and the decorrelation approximation are accurate, it should match satellite observations (not done here). In the Tropical Pacific, QCA statistics show a peak probability of clear sky at 59%, plus ~10% deep cumulus clouds (total COD > 30).~~ This histogram (blue dots) is our best estimate of the distribution of total COD from a 1D nadir perspective of all the sub-grid ICAs. The UCI J-values are calculated as the average over 4 quadrature column atmospheres (QCAs) as representatives of the ICAs. The two single-column atmosphere (SCA) models use simple averaging (COD x CF, green dots) and B-averaging (COD x $CF^{3/2}$, orange dots), which reduces the cloud fraction but assumes maximal cloud overlap. In these cases, a single J-value calculation is made with the SCA. When the clouds are simply averaged over the grid cell (~1° x 1°), the clear-sky occurrence drops to 7 % and the deep cumulus disappears. When Briegleb (1992) B-averaging is used, there is only slightly more clear sky (12 %). ~~B-~~

Both averaging ~~produces lower optical depths than simple averaging, and~~ methods also reduce the occurrence of thick cumulus. When run at lower resolution, both averages find less clear sky ~~when run at lower resolution, ,~~ while the QCA statistics are not ~~greatly~~ affected by resolution in the range 50-200 km. This averaging, of either J-values or clouds, explains why most models do not produce a single, sharp peak at rlnJ = 0.

At sufficiently high model resolution, where CF is either 0 or 1, a new problem arises because the ~~RT~~radiative transfer problem is now clearly 3D. The 1D ~~RT~~radiative transfer used here would produce a very sharp clear-sky peak in rlnJ that is not seen in CAFS. The CAFS rlnJ distribution is widened in part by TUV albedo biases, but also because it is effectively ~~an~~a weighted average of cloud conditions over 10s of km or more and thus has lower frequency of clear sky than do the 1D ICAs. The Group 1 models with large peak distributions at rlnJ~0 appear to be basically incorrect since averages over these model resolutions (>0.5°) should reduce clear-sky occurrence. There is probably a sweet spot in model resolution at about 20 km where the model statistics, even with 1D RT, should match the observed statistics.

4.4 Ocean surface albedo

We chose our Pacific blocks for this comparison to avoid large aerosol contributions and to be oceanic to avoid large variations in surface albedo. Nevertheless, the ocean surface albedo (OSA) is variable (Jin et al., 2011), but most of these models, including TUV, assume a uniform low albedo in the range of 0.05 to 0.10. For the modeled ratio J-cloudy to J-clear, using a fixed albedo is not so important since both J-values use the same albedo. For the CAFS/TUV ratio, however, it is essential to have the TUV model use the OSA that best corresponds to the sea surface conditions under the CAFS measurement. Work on the CAFS/TUV calibration seeks to achieve this zero bias, and it continues beyond the cutoff date of the ATom-1 data used here. The OSA affects our 2 J's differently: for J-O1D with peak photolysis about 305 nm, the OSA under typical conditions (SZA = 20º, surface wind = 10 m/s, chlorophyll = 0.05 mg/m3) is 0.038; while for J-NO2 with peak photolysis at 380 nm, the OSA is 0.048. OSA depends critically on the incident angle of radiation, increasing from 0.048 at 20º to 0.068 at 50º (380 nm). Rayleigh scattered light has on average larger incident angles than the solar beam for CAFS measurements and is reflected more than the direct beam. Rayleigh scattering is much more important for J-O1D than J-NO2.

The UCI standalone photolysis model was rewritten to include a lower boundary albedo that varies with angle of incident radiation, and is now designated Cloud-J version 8. In Cloud-J there are 5 incident angles on the lower surface: the direct solar beam and the 4 fixed-angle downward streams of scattered light. The ocean surface albedos (OSA) modules are adapted from the codes of Séférian et al. [2018] based on Jin et al. [2011], but we do not use their approximation for a single 'diffuse' radiation since all of Cloud-J's scattered light is resolved by zenith angle. The resulting albedo is a function of wavelength, wind speed, and chlorophyll; it is computed for each SZA and the 4 fixed scattering angles. As a test of the importance of using a more realistic OSA, we used Cloud-J v8 to compute the ratio of J with our OSA module to J using a constant fixed albedo, with both J's calculated for clear-sky. We calculate this rlnJ (log of the ratio of J-clear (OSA) to J-clear (single albedo))

for a range of SZA, wind speeds, and chlorophyll comparing to fixed albedos of 0.00, 0.06 and 0.10 as shown in Figure ~~S8~~S9. Because of the range in conditions, there is no single offset, but we have a probability distribution whose width in rlnJ due to a range of surface albedo has a magnitude that affects the interpretation of measurement-model differences. For high sun (SZA = 0º – 40º), choosing an optimal fixed albedo of 0.06 results in little mean bias, although individual errors are about ±2%. This error is based on conditions for cos(SZA) > 0.8. If the fixed albedo differs from this optimum (e.g., 0.00 or 0.10), then bias errors of 2 % to 10 % appear, and the width of the distribution expands greatly. For SZA = 40º – 80º, the optimum fixed albedo starts showing bias and has a much broader range of errors under different circumstances (wind, chlorophyll, SZA). Thus J-values calculated using unphysical, simplistic fixed ocean surface albedos can have errors of order ±10% depending on ocean surface conditions and the angular distribution of direct and scattered light at the surface. These errors will not directly affect the model results here since the cloudy-clear differences used a self-consistent albedo in each model. Overall, however, there is a need for chemistry models to implement a more physically realistic OSA.

5 Discussion

The importance of clouds in altering photolysis rates (J's) and thence tropospheric chemistry is undisputed. On a case level it is readily observed, and on a global level, every model that has included cloud scattering finds significant changes in chemical rates and budgets. For example, Spivakovsky et al.'s (2000) inclusion of cloud layers caused a shift in peak OH abundance from the boundary layer to just above it, resulting in a shift to colder temperatures (and lower reaction rates) for the oxidation of CH_4-like gases, even with the same average OH abundance. Other than single-column, idealized, off-line tests of radiative transfer methods, we have few methods to constrain ~~the~~ modeled J's under cloudy conditions.

~~The impact of clouds on J's is large, simply by looking at the mean J's (Figure 3). The modeled cloud-driven shifts range from 0 to +30 % in the free troposphere and 0 to -20 % in the boundary layer. These averages hide even larger perturbations occurring immediately above, inside and below cloud decks. The approach here is successful in developing an observed climatology of the probability distribution of cloud effects and in testing the patterns and statistics of the J's generated by global atmospheric chemistry models against it. These statistics are a more difficult and yet constructive test of models than just a mean profile of cloudy to clear. The amplitude and frequency of perturbations relative to clear sky are large, asymmetric and varying with altitude and region. Distinct classes of models have been identified.~~

The impact of clouds on J's is large, simply by looking at the profile of mean J's (Figures 1, 2, and 3); and it greatly complicates the comparison of J-values across models. The modeled mean clear-sky profiles, including CAFS TUV model (Figure 2), tend to agree within ±10% with the exception of MOCA, GISS and sometimes IFS. However, the all-sky (cloudy) profiles (Figure 1) have a much wider spread, except for J-O1D in the north Pacific for which there is inexplicably a core group of 8 models within ±10%. The observed CAFS cloudy profiles show a distinctly different profile in the north Pacific versus the tropical Pacific for both J-O1D and J-NO2 (Figure 1) and especially in the CAFS/TUV derived J-cloudy to J-clear ratios (Figure 3).

Many models follow this typical profile in the tropical Pacific (100-900 hPa, Figure 3), but some (NCAR, UCI, UCIb) show large shifts to enhanced J-values immediately above the marine boundary layer. Whether this fundamental shift in cloud regimes is robust remains uncertain, and may be resolved with the full set of ATom deployments or with careful model studies, see below.

A more informative diagnostic of cloud effects is the statistical distribution of the individual J-cloudy to J-clear ratios (rlnJ). To model clouds correctly we need to understand how frequently and by how much clouds interfere with J-values. The statistical distribution of rlnJ shows distinct patterns and classes of models. In the free troposphere (100-900 hPa), all have a sharp edge at rlnJ = 0 with hardly any diminished J-values (rlnJ < 0), but the small-cloud-effects models (GC, GFDL, GISS, GMI, UKCA) show a dominant peak at rlnJ ~ 0 while the large-cloud-effects models (IFS, MOCA, NCAR, UCI, UCIb) have extensively enhanced J-values with large fractions at +25% or more. In the marine boundary layer (surface-900 hPa), this pattern is reversed with a sharp edge for all models at rlnJ ~ +0.03, and the large-cloud-effects models showing more diminished J-values. CAFS/TUV has its own pattern, which is very broadened, but generally supports the large-cloud-effect models. If further analysis can tighten the CAFS rlnJ distribution, then we may be able to discriminate among the models in one of the classes. One robust result from the models is that large cloud effects (|rlnJ| > 0.05) are always asymmetric, splitting in sign above and below 900 hPa. If the symmetric spread in CAFS rlnJ remains robust with additional deployments and efforts to reduce CAFS-TUV inconsistencies, then we have a clear challenge for the cloud climatologies used in the chemistry models.

More work ~~is needed to improve this~~on the CAFS ~~climatology to~~/TUV data could help better discriminate among the ~~models shown~~model classes identified here. For one, we ~~probably~~ need to sample over different seasons and synoptic conditions~~, and, fortunately, the CAFS measurements from~~ to build a more robust climatology. Fortunately, the additional three deployments (ATom-2, -3, -4) will ~~naturally~~ provide these. They occur in different seasons; that is a consideration; but ~~to first order,~~ the ~~high sun,~~tropical oceanic data ~~from low latitudes~~ can probably be combined. The analysis can be extended to the Atlantic. CAFS or similar measurements from other aircraft missions could also be added. ~~The second task is to improve~~Other tasks involve tightening the spread in rlnJ by looking for potential measurement-model "noise" (e.g., aircraft-sun orientation, sun-cloud geometries) and by improving the TUV clear-sky modeling ~~so that it can use~~(e.g., a more accurate ocean surface albedo derived from observed ~~conditions (~~surface wind, chlorophyll, SZA). ~~A third~~An unresolved ~~task~~issue is how to treat aerosols, both in the models and in CAFS. If 'clear sky' includes aerosols then TUV must be able to infer an aerosol profile for all measurements, and likewise the models ~~must~~need to be careful in how they calculate cloudy-to-clear. Fortunately for most of the oceanic ATom measurements, aerosol optical depths are small, but where they are large (e.g., Saharan dust events) the daily satellite mapping should provide adequate coverage for the TUV modeling. Developing these cloudy-to-clear J-value statistics over land will be more difficult due to the higher inherent variability in albedo and aerosol profiles.

More effort is needed from the modeling community to characterize the key factors driving these model differences in photolysis rates under realistic, cloudy conditions. This might include sensitivity runs that address aerosol and surface albedo impacts for each model. We would also need a better characterization of the cloud distributions used in chemistry models, including comparison with satellite climatologies (Cesana and Waliser, 2016; Ham et al., 2017), to understand how cloud fraction and overlap affects the J's used in the photochemical calculation of a column atmosphere. ~~A~~Models can help assess the ATom CAFS statistics for representativeness by checking on flight routing, multiple days, or different years.

The 3D nature of the radiation field measured by aircraft presents a more fundamental ~~difficulty with this model-measurement comparison remains: the~~challenge. The observations average over cloud fields out to 10s of km, and ~~hence over the oceans have frequent cloud influence~~even if the atmospheric column at the aircraft is clear, neighboring clouds alter J-values. The chemical models are coarse resolution compared with the CAFS measurements and average over wider range of cloud fields, almost eliminating the occurrence of clear-sky conditions. Even if they calculate a distribution of J-values for the cloud statistics in a column (like Cloud-J), they combine these to deliver a single average J-value for the chemistry module, again reducing the occurrence of clear-sky J-values. Thus, the result above (i.e., that 5 models have about 50% nearly-clear-sky J-values down to the surface) is inexplicable unless they have column optical depths of 0.3 or very small effective cloud fractions. At some model resolution, probably of order 10s km, the CAFS measurements may be a statistical representation over that grid; and our comparisons, even with 1D ~~RT averages~~radiative transfer over a range of ICAs, may be more consistent. At these scales, there remains the problem of a strong zenith angle dependence (Tompkins and Giuseppe, 2007). Super-high resolution models (~1 km) are becoming available in regional or nested-grid models (Kendon et al., 2012; Schwartz, 2014; Berthou et al., 2018), and one might hope that our problem is now solved because each single column atmosphere (SCA) explicitly resolves cloud overlap with each grid cell being either cloudy or clear. The calculation of photolysis and solar heating rates is not simplified, however, because now the SCAs interact with neighbors. To calculate the correct rates at any location, or even the average over a region, ~~we must be able to~~would require that we calculate the ratio of cloudy to clear over a 20-km domain of cloud-resolved grid cells.

~~More effort is needed from the modeling community to characterize the key factors driving these model differences in photolysis rates under realistic, cloudy conditions. This might include some sensitivity runs that address aerosol and surface albedo impacts for each model. We would also need a better characterization of the cloud distributions used in chemistry models, including comparison with satellite climatologies (Cesana and Waliser, 2016; Ham et al., 2017), to understand how cloud fraction and overlap affects the J's used in the photochemical calculation of a column atmosphere. Models can assess the importance of CAFS representativeness and the robustness of the statistics by checking on multiple days or different years. Another important model-CAFS collaboration should explore the actual flight paths and cloud fields to see if certain cloud conditions are avoided or over-sampled.~~

Data availability: The data sets used here for the plots and analysis are extensive (~10 GB) and will be archived at the Oak Ridge National Laboratory DAAC under the doi: Hall et al. (2018) https://doi.org/10.3334/ORNLDAAC/xxxx. The data analysis codes, in terms of MATLAB scripts, are archived there also.

Author contributions: SRH and MJP designed this analysis. MJP developed the codes to analyse, compare and plot the data. SRH and KU performed the CAFS analysis and contributed those data. All other others ran the prescribed model experiments and contributed their model data. MJP and SRH prepared the manuscript with review and edits from all other co-authors.

Competing interests: The authors declare that they have no conflict of interest.

Acknowledgments

This work is supported by the ATom investigation under National Aeronautics and Space Administration's Earth Venture program (grants NNX15AJ23G, NNX15AG57A, NNX15AG58A~~)~~., NNX15AG71A). The National Center for Atmospheric Research is sponsored by the National Science Foundation. The UKCA simulations used the NEXCS High Performance Computing facility funded by the U.K. Natural Environment Research Council and delivered by the Met Office. ATA and NLA thank NERC through NCAS and through the ACSIS project which has enabled this work. VH acknowledges funding from the Copernicus Atmosphere Monitoring Service (CAMS). AMF acknowledges L.W. Horowitz (NOAA GFDL) for technical guidance with AM3. The data used in this work and supporting its conclusions are available at Hall et al. (2018) https://doi.org/10.3334/ORNLDAAC/xxxx.

References

Arteta, J. and Flemming, J.: "Documentation of C-IFS-MOCAGE." http://www.gmes-atmosphere.eu/documents/macciii/deliverables/grg/MACCIII_GRG_DEL_D_24.3_C-IFS_MOCAGE_final.pdf, 2015.

Atkinson, R., Baulch, D. L., Cox, R. A., Crowley, J. N., Hampson, R. F., Hynes, R. G., Jenkin, M. E., Rossi, M. J. and Troe, J.: Evaluated kinetic and photochemical data for atmospheric chemistry: Volume I - gas phase reactions of Ox, HOx, NOx and SOx species, Atmos. Chem. Phys., 4, 1461-1738, doi: 10.5194/acp-4-1461-2004, 2004.

ATom, Measurements and modeling results from the NASA Atmospheric Tomography Mission, https://espoarchive.nasa.gov/archive/browse/atom, doi: 10.5067/Aircraft/ATom/TraceGas_Aerosol_Global_Distribution, 2017.

Barker, H. W.: Overlap of fractional cloud for radiation calculations in GCMs: A global analysis using CloudSat and CALIPSO data, J. Geophys. Res., 113, D00A01, doi:10.1029/2007JD009677, 2008a.

Barker, H. W.: Representing cloud overlap with an effective decorrelation length: An assessment using CloudSat and CALIPSO data, J. Geophys. Res., 113, D24205, doi:10.1029/2008JD010391, 2008b.

Barker, H. W., M. P. Jerg, T. Wehr, S. Kato, D. P. Donovan, and R. J. Hogan: A 3D cloud-construction algorithm for the EarthCARE satellite mission. Quart. J. Roy. Meteor. Soc., 137, 1042–1058, doi:10.1002/qj.824, 2011..

Berthou, S., Kendon, E.J., Chan, S.C., Ban, N., Leutwyler, D., Schär, C., and Fosser, G.: Pan-European climate at convection-permitting scale: a model intercomparison study. Climate Dynamics 5, doi: 10.1007/s00382-018-4114-6, 2018.

Bian, H. S., Prather, M. J., and Takemura, T.: Tropospheric aerosol impacts on trace gas budgets through photolysis, J Geophys Res-Atmos, 108, -, Artn 4242 Doi 10.1029/2002jd002743, 2003.

Brasseur, G. P., D. A. Hauglustaine, S. Walters, P. J. Rasch, J.-F. Müller, C. Granier, and X. X. Tie: MOZART, a global chemical transport model for ozone and related chemical tracers: 1. Model description, J. Geophys. Res., 103(D21), 28265–28289, doi:10.1029/98JD02397, 1998.

Briegleb, B. P.: Delta-Eddington approximation for solar radiation in the NCAR community climate model, J. Geophys. Res., 97, 7603–7612, 1992.

Burkholder, J. B., S. P. Sander, J. Abbatt, J. R. Barker, R. E. Huie, C. E. Kolb, M. J. Kurylo, V. L. Orkin, D. M. Wilmouth, and P. H. Wine: Chemical kinetics and photochemical data for use in atmospheric studies, Evaluation No. 18, JPL Publication 15-10, Jet Propul. Lab., Pasadena, Calif., http://jpldataeval.jpl.nasa.gov, 2015.

Cesana, G. and Waliser, D. E.: Characterizing and understanding systematic biases in the vertical structure of clouds in CMIP5/CFMIP2 models,. Geophys. Res. Lett., 43, 10,538–10,546, doi:10.1002/2016GL070515, 2016.

Chang, J. S., Brost, R. A., Isaksen, I. S. A., Madronich, S., Middleton, P., Stockwell, W. R., and Walcek, C. J.: A three-dimensional Eulerian acid deposition model: Physical concepts and formulation, J. Geophys. Res., 92, 14,681–14,700, 1987.

Crawford, J., Shetter, R. E., Lefer, B., Cantrell, C., Junkermann, W., Madronich, S., and Calvert, J.: Cloud impacts on UV spectral actinic flux observed during the International Photolysis Frequency Measurement and Model Intercomparison (IPMMI), J. Geophys. Res., 108(D16), 8545, doi:10.1029/2002JD002731, 2003.

Donner, L. J., Wyman, B. L., Hemler, R. S., Horowitz, L. W., Ming, Y., Zhao, M., Golaz, J. C., Ginoux, P., Lin, S. J., Schwarzkopf, M. D., Austin, J., Alaka, G., Cooke, W. F., Delworth, T. L., Freidenreich, S. M., Gordon, C. T., Griffies, S. M., Held, I. M., Hurlin, W. J., Klein, S. A., Knutson, T. R., Langenhorst, A. R., Lee, H. C., Lin, Y. L., Magi, B. I., Malyshev, S. L., Milly, P. C. D., Naik, V., Nath, M. J., Pincus, R., Ploshay, J. J., Ramaswamy, V., Seman, C. J., Shevliakova, E., Sirutis, J. J., Stern, W. F., Stouffer, R. J., Wilson, R. J., Winton, M., Wittenberg, A. T., and Zeng, F. R.: The Dynamical Core, Physical Parameterizations, and Basic Simulation Characteristics of the Atmospheric Component AM3 of the GFDL Global Coupled Model CM3, J Climate, 24, 3484-3519, doi 10.1175/2011jcli3955.1, 2011.

Duncan, B.N., Strahan, S.E., Yoshida, Y., Steenrod, S.D., and Livesey, N.: Model study of cross-tropopause transport of biomass burning pollution, Atmos. Chem. Phys., 7, 3713-3736, 2007.

Feng, Y., Penner, J. E., Sillman, S., and Liu, X.: Effects of cloud overlap in photochemical models, J. Geophys. Res., 109, D04310, doi:10.1029/2003JD004040, 2004.

Flemming, J., Huijnen, V., Arteta, J., Bechtold, P., Beljaars, A., Blechschmidt, A.-M., Diamantakis, M., Engelen, R. J., Gaudel, A., Inness, A., Jones, L., Josse, B., Katragkou, E., Marecal, V., Peuch, V.-H., Richter, A., Schultz, M. G., Stein, O., and Tsikerdekis, A.: Tropospheric chemistry in the Integrated Forecasting System of ECMWF, Geosci. Model Dev., 8, 975-1003, doi: 10.5194/gmd-8-975-2015, 2015.

Gelaro, R., McCarty, W., Suárez, M. J., Todling, R., Molod, A., Takacs, L., Randles, C. A., Darmenov, A., Bosilovich, M. G., Reichle, R., Wargan, K., Coy, L., Cullather, R., Draper, C., Akella, S., Buchard, V., Conaty, A., da Silva, A. M., Gu, W., Kim, G.-K., Koster, R., Lucchesi, R., Merkova, D., Nielsen, J. E., Partyka, G., Pawson, S., Putman,W., Rienecker, M., Schubert, S. D., Sienkiewicz, M., and Zhao, B.: The Modern-Era Retrospective Analysis for Research and Applications, Version 2 (MERRA-2), J. Climate, 30, 5419–5454, https://doi.org/10.1175/JCLI-D-16-0758.1, 2017.

Guth, J., Josse, B., Marécal, V., Joly, M., and Hamer, P.: First implementation of secondary inorganic aerosols in the MOCAGE version R2.15.0 chemistry transport model, Geosci. Model Dev., 9, 137-160, https://doi.org/10.5194/gmd-9-137-2016, 2016.

Ham, S.-H., Kato, S., Rose, F. G., Winker, D., L'Ecuyer, T., Mace, G.G., Painemal, D., Sun-Mack, S., Chen, Y., Miller, C., and Walter F.: Cloud Occurrences and Cloud Radiative Effects (CREs) from CERES-CALIPSO-CloudSat-MODIS (CCCM) and CloudSat Radar-Lidar (RL) Products, Journal of Geophysical Research: Atmospheres, 122(16), 8852–8884. doi: 10.1002/2017JD026725, 2017.

Hofzumahaus, A., Lefer, B. L., Monks, P. S., Hall, S. R., Kylling, A., Shetter, B. M. R. E., Junkermann, W., Bais, A., Calvert, J. G., Cantrell, C. A., Madronich, S., Edwards, G. D., Kraus, A., M¨uller, M., Bohn, B., Schmitt, R., Johnston, P., McKenzie, R., Frost, G. J., Griffioen, E., Krol, M., Martin, T., Pfister, G., Roth, E. P., Ruggaber, A., Swartz, W. H., Lloyd, S. A., and Van Weele, M.: Photolysis frequency of O_3 to $O(^1D)$: Measurements and modeling during the International Photolysis Frequency Measurement and Modeling Intercomparison (IPMMI), J. Geophys. Res., 109, D08S90, doi:10.1029/2003JD004333, 2004.

Hogan, R.J. and Illingworth, A.J.: Deriving cloud overlap statistics from radar, Q.J.R.Meteorol.Soc. 126: 2903-2909,2000.

Holmes, C.D., Prather, M.J., Søvde, A.O., and Myhre, G.: Future methane, hydroxyl, and their uncertainties: key climate and emission parameters for future predictions, Atmos. Chem. Phys., 13, 285–302, doi:10.5194/acp-13-285-2013, 2013.

Jin, Z., Qiao, Y., Wang, Y., Fang, Y., and Yi, W.: A new parameterization of spectral and broadband ocean surface albedo, Opt. Express, 19, 26429–26443, 2011.

Kendon, E. J., Roberts, N.M., Senior, C.A., and Roberts, M.J.: Realism of rainfall in a very high-resolution regional climate model. J. Climate, 25: 5791–5806, doi 10.1175/JCLI-D-11-00562.1, 2012.

Kim, H.C., Lee, P., Ngan, F.,Tang, Y., Yoo, H.L., and Pan L.: Evaluation of modeled surface ozone biases as a function of cloud cover fraction, Geosci. Model Dev., 8, 2959–2965, 2015, doi:10.5194/gmd-8-2959-2015, 2015.

Lamarque, J. F., Shindell, D. T., Josse, B., Young, P. J., Cionni, I., Eyring, V., Bergmann, D., Cameron-Smith, P., Collins, W. J., Doherty, R., Dalsoren, S., Faluvegi, G., Folberth, G., Ghan, S. J., Horowitz, L. W., Lee, Y. H., MacKenzie, I. A., Nagashima, T., Naik, V., Plummer, D., Righi, M., Rumbold, S. T., Schulz, M., Skeie, R. B., Stevenson, D. S., Strode, S., Sudo, K., Szopa, S., Voulgarakis, A., and Zeng, G.: The Atmospheric Chemistry and Climate Model Intercomparison Project (ACCMIP): overview and description of models, simulations and climate diagnostics, Geosci Model Dev, 6, 179-206, DOI 10.5194/gmd-6-179-2013, 2013.

Lefer, B. L., Shetter, R.E., Hall, S.R., Crawford, J.H., and Olson, J.R.: Impact of clouds and aerosols on photolysis frequencies and photochemistry during TRACE-P: 1. Analysis using radiative transfer and photochemical box models, J. Geophys. Res., 108(D21), 8821, doi:10.1029/2002JD003171, 2003.

Levelt, P. F., van den Oord, G. H. J., Dobber, M. R., Malkki, A., Visser, H., de Vries, J., Stammes, P., Lun- dell, J. O. V., and Saari, H.: The ozone monitoring instrument, IEEE T. Geosci. Remote, 44, 1093–1101, https://doi.org/10.1109/TGRS.2006.872333, 2006.

Li, J., Huang, J., Stamnes, K., Wang, T., Lv, Q., and Jin, H.: A global survey of cloud overlap based on CALIPSO and CloudSat measurements, Atmos. Chem. Phys., 15, 519-536, https://doi.org/10.5194/acp-15-519-2015, 2015.

Li, J., Mao, J., Fiore, A. M., Cohen, R. C., Crounse, J. D., Teng, A. P., Wennberg, P. O., Lee, B. H., Lopez-Hilfiker, F. D., Thornton, J. A., Peischl, J., Pollack, I. B., Ryerson, T. B., Veres, P., Roberts, J. M., Neuman, J. A., Nowak, J. B., Wolfe, G. M., Hanisco, T. F., Fried, A., Singh, H. B., Dibb, J., Paulot, F., and Horowitz, L. W.: Decadal changes in summertime reactive oxidized nitrogen and surface ozone over the Southeast United States, Atmos. Chem. Phys., 18, 2341-2361, https://doi.org/10.5194/acp-18-2341-2018, 2018.

Lin, J.-T., Liu, Z., Zhang, Q., Liu, H., Mao, J., and Zhuang, G.: Modeling uncertainties for tropospheric nitrogen dioxide columns affecting satellite-based inverse modeling of nitrogen oxides emissions, Atmos. Chem. Phys., 12, 12255-12275, https://doi.org/10.5194/acp-12-12255-2012, 2012.

Liu, H., Crawford, J.H., Pierce, R.B., Norris, P.M., Platnick, S.E., Chen, G., Logan, J.A.,Yantosca, R.M., Evans, M.J., Kittaka, C., Feng, Y., and Tie, X.: Radiative effect of clouds on tropospheric chemistry in a global three-dimensional chemical transport model, J. Geophys. Res., 111, D20303, doi:10.1029/2005JD006403, 2006.

Liu, H., Crawford, J.H., Considine, D.B., Platnick, S., Norris, P.M., Duncan, B.N., Pierce, R.B., Chen, G., and Yantosca, R.M.: Sensitivity of photolysis frequencies and key tropospheric oxidants in a global model to cloud vertical distributions and optical properties, J. Geophys. Res., 114, D10305, doi:10.1029/2008JD011503, 2009.

Logan, J. A., Prather, M. J., Wofsy, S. C., and McElroy, M. B.: Tropospheric Chemistry - a Global Perspective, Journal of Geophysical Research-Oceans and Atmospheres, 86, 7210-7254, Doi 10.1029/Jc086ic08p07210, 1981.

M&M, The Atmospheric Effects of Stratospheric Aircraft: Report of the 1992 Models and Measurements Workshop, NASA Ref. Publ. 1292, M.J. Prather and E.E. Remsberg, Eds.), Satellite Beach, FL, Volumes: I-II-II, 144pp–268pp–352pp, 1993.

Madronich S. and Flocke S.: The Role of Solar Radiation in Atmospheric Chemistry. In: Boule P. (eds) Environmental Photochemistry. The Handbook of Environmental Chemistry (Reactions and Processes), vol 2 / 2L. Springer, Berlin, Heidelberg, 1999.

Madronich, S.: Photodissociation in the atmosphere: 1. Actinic flux and the effect of ground reflections and clouds, J. Geophys. Res., 92, 9740 – 9752, 1987.

Mao, J., Horowitz, L.W., Naik, V., Fan, S., Liu, J., Fiore, A.M.: Sensitivity of tropospheric oxidants to biomass burning emissions: implications for radiative forcing. Geophysical Research Letters, 40(6), doi:10.1002/grl.50210, 2013.

Martin, R. V., Jacob, D. J., Yantosca, R. M., Chin, M., and Ginoux, P.: Global and regional decreases in tropospheric oxidants from photochemical effects of aerosols, J Geophys Res-Atmos, 108, -, Artn 4097 Doi 10.1029/2002jd002622, 2003.

Miller, S.D., J.M. Forsythe, P.T. Partain, J.M. Haynes, R.L. Bankert, M. Sengupta, C. Mitrescu, J.D. Hawkins, and T.H. Vonder Haar: Estimating three-dimensional cloud structure via statistically blended satellite observations. J. Appl. Meteor. Climatol., 53, 437–455, doi:10.1175/JAMC-D-13-070.1, 2014.

Morcrette, J.-J. and Fouquart, Y.: The overlapping of cloud layers in shortwave radiation parameterizations, J. Atmos. Sci., 43(4), 321–328, 1986.

Morgenstern, O., Hegglin, M. I., Rozanov, E., O'Connor, F. M., Abraham, N. L., Akiyoshi, H., Archibald, A. T., Bekki, S., Butchart, N., Chipperfield, M. P., Deushi, M., Dhomse, S. S., Garcia, R. R., Hardiman, S. C., Horowitz, L. W., Jockel, P., Josse, B., Kinnison, D., Lin, M. Y., Mancini, E., Manyin, M. E., Marchand, M., Marecal, V., Michou, M., Oman, L. D., Pitari, G., Plummer, D. A., Revell, L. E., Saint-Martin, D., Schofield, R., Stenke, A., Stone, K., Sudo, K., Tanaka, T. Y., Tilmes, S., Yamashita, Y., Yoshida, K., and Zeng, G.; Review of the global models used within phase 1 of the Chemistry-Climate Model Initiative (CCMI), Geosci Model Dev, 10, 639-671, 10.5194/gmd-10-639-2017, 2017.

Nack, M. L. and Green, A. E. S.: Influence of clouds, haze, and smog on the middle ultraviolet reaching the ground, Appl. Opt., 13, 2405– 2415, 1974.

Naik, V., Horowitz, L. W., Fiore, A. M., Ginoux, P., Mao, J. Q., Aghedo, A. M., and Levy, H.: Impact of preindustrial to present-day changes in short-lived pollutant emissions on atmospheric composition and climate forcing, J Geophys Res-Atmos, 118, 8086-8110, 10.1002/jgrd.50608, 2013.

Neu, J. L., Prather, M.J., and Penner, J.E.: Global atmospheric chemistry: Integrating over fractional cloud cover, J. Geophys. Res., 112, D11306, doi:10.1029/2006JD008007, 2007.

O'Connor, F. M., Johnson, C. E., Morgenstern, O., Abraham, N. L., Braesicke, P., Dalvi, M., Folberth, G. A., Sanderson, M. G., Telford, P. J., Voulgarakis, A., Young, P. J., Zeng, G., Collins, W. J., and Pyle, J. A.: Evaluation of the new UKCA climate-composition model – Part 2: The Troposphere, Geosci. Model Dev., 7, 41-91, https://doi.org/10.5194/gmd-7-41-2014, 2014.

Olson, J., Prather, M., Berntsen, T., Carmichael, G., Chatfield, R., Connell, P., Derwent, R., Horowitz, L., Jin, S. X., Kanakidou, M., Kasibhatla, P., Kotamarthi, R., Kuhn, M., Law, K., Penner, J., Perliski, L., Sillman, S., Stordal, F., Thompson, A., and Wild, O.: Results from the Intergovernmental Panel on Climatic Change Photochemical Model Intercomparison (PhotoComp), J Geophys Res-Atmos, 102, 5979-5991, 1997.

Palancar, G. G., Shetter, R. E., Hall, S. R., Toselli, B. M., and Madronich, S.: Ultraviolet actinic flux in clear and cloudy atmospheres: model calculations and aircraft-based measurements, Atmos. Chem. Phys., 11, 5457-5469, https://doi.org/10.5194/acp-11-5457-2011, 2011.

Petropavlovskikh, I., Shetter, R., Hall, S., Ullmann, K., Bhartia, P.K.: Algorithm for the charge-coupled-device scanning actinic flux spectroradiometer ozone retrieval in support of the Aura satellite validation, J. Appl. Remote Sens., 1, 013540, doi:10.1117/1.2802563, 2007.

PhotoComp: Chapter 6 - Stratospheric Chemistry SPARC Report No. 5 on the Evaluation of Chemistry-Climate Models 194-202, 2010.

Pincus, R., Barker, H. W., and Morcrette, J. J.: A fast, flexible, approximate technique for computing radiative transfer in inhomogeneous cloud fields, J. Geophys. Res.-Atmos., 108, D4376, https://doi.org/10.1029/2002jd003322, 2003.

Prather, M.J.: Photolysis rates in correlated overlapping cloud fields: Cloud-J 7.3c, Geosci. Model Dev., 8, 2587-2595, doi:10.5194/gmd-8-2587-2015, 2015.

Prather, M. J., Zhu, X., Flynn, C. M., Strode, S. A., Rodriguez, J. M., Steenrod, S. D., Liu, J., Lamarque, J.-F., Fiore, A. M., Horowitz, L. W., Mao, J., Murray, L. T., Shindell, D. T., and Wofsy, S. C.: Global atmospheric chemistry – which air matters, Atmos. Chem. Phys., 17, 9081-9102, https://doi.org/10.5194/acp-17-9081-2017, 2017.

Prather, M. J., Flynn, C. M., Zhu, X., Steenrod, S. D., Strode, S. A., Fiore, A. M., Correa, G., Murray, L. T., and Lamarque, J.-F.: How well can global chemistry models calculate the reactivity of short-lived greenhouse gases in the remote troposphere, knowing the chemical composition, Atmos. Meas. Tech., 11, 2653-2668, https://doi.org/10.5194/amt-11-2653-2018, 2018.

Rienecker, M. M., Suarez, M. J., Gelaro, R., Todling, R., Bacmeister, J., Liu, E., Bosilovich, M. G., Schubert, S. D., Takacs, L., Kim, G.-K., Bloom, S., Chen, J., Collins, D., Conaty, A., da Silva, A., Gu, W., Joiner, J., Koster, R. D., Lucchesi, R., Molod, A., Owens, T., Pawson, S., Pegion, P., Redder, C. R., Reichle, R., Robertson, F. R., Ruddick, A. G., Sienkiewicz, M., and Woollen, J.: MERRA: NASA's Modern-Era Retrospective Analysis for Research and Application, J. Climate, 24, 3624–3648. doi:10.1175/JCLI-D-11-00015.1, 2011.

Ryu, Y.-H., Hodzic, A., Descombes, G., Hall, S., Minnis, P., Spangenberg, D., Ullmann, K., and Madronich, S.: Improved modeling of cloudy-sky actinic flux using satellite cloud retrievals, Geophys. Res. Lett., 44, doi:10.1002/2016GL071892, 2017.

Schmidt, G. A., Kelley, M., Nazarenko, L., Ruedy, R., Russell, G.L., Aleinov, I., Bauer, M., Bauer, S. E., Bhat, M. K., Bleck, R., Canuto, V., Chen, Y., Cheng, Y., Clune, T. L., Del Genio, A., de Fainchtein, R., Faluvegi, G., Hansen, J. E., Healy, R. J., Kiang, N. Y., Koch, D., Lacis, A. A., LeGrande, A. N., Lerner, J., Lo, K. K., Matthews, E. E., Menon, S., Miller, R. L., Oinas, V., Oloso, A. O., Perlwitz, J. P., Puma, M. J., Putman, W. M., Rind, D., Romanou, A., Sato, M., Shindell, D. T., Sun, S., Syed, R. A., Tausnev, N., Tsigaridis, K., Unger, N., Voulgarakis, A., Yao, M.-S., and Zhang, J.: Configuration and assessment of the GISS ModelE2 contributions to the CMIP5 archive, J. Adv. Model. Earth Syst., 6, 141–184, doi:10.1002/2013MS000265, 2014.

Schwartz, C.S.: Reproducing the September 2013 record-breaking rainfall over the Colorado front range with high-resolution WRF forecasts. Weather Forecast 29:393–402. doi: 10.1175/WAF-D-13-00136.1, 2014.

Séférian, R., Baek, S., Boucher, O., Dufresne, J.-L., Decharme, B., Saint-Martin, D., and Roehrig, R.: An interactive ocean surface albedo scheme (OSAv1.0): formulation and evaluation in ARPEGE-Climat (V6.1) and LMDZ (V5A), Geosci. Model Dev., 11, 321-338, https://doi.org/10.5194/gmd-11-321-2018, 2018.

Shetter, R. E. and Müller, M.: Photolysis frequency measurements using actinic flux spectroradiometry during the PEM-Tropics mission: Instrumentation description and some results, J. Geophys. Res., 104(D5), 5647–5661, doi:10.1029/98JD01381, 1999.

Shetter, R. E., Cinquini, L., Lefer, B.L., Hall, S.R., and Madronich, S.: Comparison of airborne measured and calculated spectral actinic flux and derived photolysis frequencies during the PEM Tropics B mission, J. Geophys. Res., 107, 8234, doi:10.1029/2001JD001320, 2002.

Shetter, R. E., Junkermann, W., Swartz, W. H., Frost, G. J., Crawford, J. H., Lefer, B. L., Barrick, J. D., Hall, S. R., Hofzumahaus, A., Bais, A., Calvert, J. G., Cantrell, C. A., Madronich, S., Mueller, M., Kraus, A., Monks, P. S., Edwards, G. D., McKenzie, R., Johnston, P., Schmitt, R., Griffioen, E., Krol, M., Kylling, A., Dickerson, R. R., Lloyd, S. A., Martin, T., Gardiner, B., Mayer, B., Pfister, G., Roeth, E. P., Koepke, P., Ruggaber, A., Schwander, H., and van Weele, M.: Photolysis frequency of NO2: Measurement and modeling during the International Photolysis Frequency Measurement and Modeling Intercomparison (IPMMI), J. Geophys. Res., 108, doi:10.1029/2002JD002932, 2003.

Shindell, D., Kuylenstierna, J. C. I., Vignati, E., van Dingenen, R., Amann, M., Klimont, Z., Anenberg, S. C., Muller, N., Janssens-Maenhout, G., Raes, F., Schwartz, J., Faluvegi, G., Pozzoli, L., Kupiainen, K., Hoglund-Isaksson, L., Emberson, L., Streets, D., Ramanathan, V., Hicks, K., Oanh, N. T. K., Milly, G., Williams, M., Demkine, V., and Fowler, D.: Simultaneously Mitigating Near-Term Climate Change and Improving Human Health and Food Security, Science, 335, 183–189, https://doi.org/10.1126/science.1210026, 2012.

Spivakovsky, C. M., Logan, J. A., Montzka, S. A., Balkanski, Y. J., Foreman-Fowler, M., Jones, D. B. A., Horowitz, L. W., Fusco, A. C., Brenninkmeijer, C. A. M., Prather, M. J., Wofsy, S. C., McElroy, M. B.: Three-dimensional climatological distribution of tropospheric OH: Update and evaluation, J. Geophys.Res., 105(D7): 8931-8980, 2000.

Strahan, S.E., Douglass, A.R., and Newman, P.A.: The contributions of chemistry and transport to low Arctic ozone in March 2011 derived from Aura MLS Observations, J. Geophys. Res., 118, 1563-1576, doi:10.1002/jgrd.50181, 2013.

Sun, Z. and Rikus, L.: Parametrization of effective sizes of cirrus-cloud particles and its verification against observations. Q.J.R. Meteorol. Soc., 125: 3037–3055. doi:10.1002/qj.49712556012, 1999.

Sun, Z.: Reply to comments by Greg M. McFarquhar on 'Parametrization of effective sizes of cirrus-cloud particles and its verification against observations'. (October B, 1999, 125, 3037–3055). Q.J.R. Meteorol. Soc., 127: 267–271. doi:10.1002/qj.49712757116, 2001.

Telford, P. J., Abraham, N. L., Archibald, A. T., Braesicke, P., Dalvi, M., Morgenstern, O., O'Connor, F. M., Richards, N. A. D., and Pyle, J. A.: Implementation of the Fast-JX Photolysis scheme (v6.4) into the UKCA component of the MetUM chemistry-climate model (v7.3), Geosci. Model Dev., 6, 161-177, https://doi.org/10.5194/gmd-6-161-2013, 2013.

Tilmes, S., Lamarque, J.-F., Emmons, L. K., Kinnison, D. E., Marsh, D., Garcia, R. R., Smith, A. K., Neely, R. R., Conley, A., Vitt, F., Val Martin, M., Tanimoto, H., Simpson, I., Blake, D. R., and Blake, N.: Representation of the Community Earth System Model (CESM1) CAM4-chem within the Chemistry-Climate Model Initiative (CCMI), Geosci. Model Dev., 9, 1853-1890, https://doi.org/10.5194/gmd-9-1853-2016, 2016.

Tompkins, A., and Giuseppe, F.D.: Generalizing Cloud Overlap Treatment to Include Solar Zenith Angle Effects on Cloud Geometry, J. Atmos.Sci. 64:2116-2125, 2007.

Tsushima, Y., Brient, F., Klein, S. A., Konsta, D., Nam, C. C., Qu, X., Williams, K. D., Sherwood, S. C., Suzuki, K., and Zelinka, M. D.: The Cloud Feedback Model Intercomparison Project (CFMIP) Diagnostic Codes Catalogue – metrics, diagnostics and methodologies to evaluate, understand and improve the representation of clouds and cloud feedbacks in climate models, Geosci. Model Dev., 10, 4285-4305, doi: 10.5194/gmd-10-4285-2017, 2017.

Veefkind, J.P., Haan, J.F., Brinksma, E.J., Kroon, M., and Levelt, P.F.: Total ozone from the ozone monitoring instrument (OMI) using the DOAS technique. IEEE Transactions on Geoscience and Remote Sensing, 44, 1239-1244, 2006.

Walters, D., Boutle, I., Brooks, M., Melvin, T., Stratton, R., Vosper, S., Wells, H., Williams, K., Wood, N., Allen, T., Bushell, A., Copsey, D., Earnshaw, P., Edwards, J., Gross, M., Hardiman, S., Harris, C., Heming, J., Klingaman, N., Levine, R., Manners, J., Martin, G., Milton, S., Mittermaier, M., Morcrette, C., Riddick, T., Roberts, M., Sanchez, C., Selwood, P., Stirling, A., Smith, C., Suri, D., Tennant, W., Vidale, P. L., Wilkinson, J., Willett, M., Woolnough, S., and Xavier, P.: The Met Office Unified Model Global Atmosphere 6.0/6.1 and JULES Global Land 6.0/6.1 configurations, Geosci. Model Dev., 10, 1487-1520, https://doi.org/10.5194/gmd-10-1487-2017, 2017.

Wild, O., Zhu, X., and Prather, M. J.: Fast-J: Accurate simulation of in- and below-cloud photolysis in tropospheric chemical models, J Atmos Chem, 37, 245-282, 2000.

Williams, J. E., Landgraf, J., Bregman, A., and Walter, H. H.: A modified band approach for the accurate calculation of online photolysis rates in stratospheric-tropospheric Chemical Transport Models, Atmos. Chem. Phys., 6, 4137-4161, https://doi.org/10.5194/acp-6-4137-2006, 2006.

Williams, J. E., Strunk, A., Huijnen, V., and van Weele, M.: The application of the Modified Band Approach for the calculation of on-line photodissociation rate constants in TM5: implications for oxidative capacity, Geosci. Model Dev., 5, 15-35, doi:10.5194/gmd-5-15-2012, 2012.

Williams, K. D. and Bodas-Salcedo, A.: A multi-diagnostic approach to cloud evaluation, Geosci. Model Dev., 10, 2547-2566, doi: 10.5194/gmd-10-2547-2017, 2017.

Wofsy, S.~~-~~C., S. Afshar, H.M. Allen, E. Apel, E.~~,~~C. Asher, B. Barletta, J. Bent, H. Bian, B.C. Biggs, D.R. Blake, ~~D. R.,~~N. Blake, I. Bourgeois, C.A. Brock, ~~C. A.,~~W.H. Brune, J.W. ~~H.,~~Budney, T.P. Bui, ~~T. P.,~~A. Butler, P. Campuzano-Jost, C.S. Chang, M. Chin, R. Commane, G. Correa, J.D. Crounse, P. D. Cullis, B.C. Daube, ~~B. C.,~~D.A. Day, J.M. Dean-Day, J.E. Dibb, J.~~E.,~~P. DiGangi, G.S. Diskin, ~~G. S., Elkiins, J. W.,~~M. Dollner, J.W. Elkins, F. Erdesz, A.M. Fiore, C.M. Flynn, K. Froyd, ~~K.,~~D.W. Gesler, S.R. Hall, ~~S. R.,~~T.F. Hanisco, ~~T. F.,~~R.A. Hannun, A.J. Hills, E.J. Hintsa, A. Hoffman, R.S. Hornbrook, L.G. Huey, S. Hughes, J.L.~~G.,~~ Jimenez, ~~J. L.,~~B.J. Johnson, J.M. Katich, R. Keeling, M.J. Kim, A. Kupc, L.R. Lait, J.-F. Lamarque, J. Liu, K. McKain, ~~K.,~~R.J. Mclaughlin, S. Meinardi, D.O. Miller, S.A. Montzka, ~~S. A.,~~F.L. Moore, E.J. Morgan, D.M. Murphy, L.T. Murray, B.A. Nault, J.A. Neuman, P.A. Newman, J.M. Nicely, X. Pan, W. Paplawsky, J. Peischl, M.J. Prather, D.J. Price, E. Ray, J.M. Reeves, M. Richardson, A.W. Rollins, K.H. Rosenlof, T.B. Ryerson, ~~T. B.,~~E. Scheuer, G.P. Schill, J.C. Schroder, J.P. Schwarz, J.~~P.,~~M. St.Clair, S.D. Steenrod, B.B. Stephens, ~~B. B.,~~S.A. Strode, C. Sweeney, D. Tanner, A.P. Teng, A.B. Thames, C.R. Thompson, K. Ullmann, P.R. Veres, N. Vieznor, N.L. Wagner, A. Watt, R. Weber, B. Weinzierl, ~~B., and~~P. Wennberg, ~~P.:~~C.J. Williamson, J.C. Wilson, G.M. Wolfe, C.T. Woods, and L.H. Zeng. 2018. ATom: Merged Atmospheric Chemistry,

Trace Gases, and Aerosols. ORNL DAAC, Oak Ridge, Tennessee, USA, available at: https://doi.org/10.3334/ORNLDAAC/1581, last access: ~~30 April~~25 October 2018.

Table 1. Modeling photolysis and cloud fields				
short name	long name	Cloud data (resolution) and date	J-values and cloud fraction (CF) treatment	Model references, including J-values
GC	GEOS-Chem	Cloud ~~fraction, liquid and ice water,~~CF+OD from MERRA-2; GC v11_01. (2.5ºx2.0º~~)~~). 2013 Aug 16	Fast-J* v7.0, single column, Briegleb averaging**	Gelaro et al., 2017; Liu et al., 2006, 2009.
GFDL	GFDL AM3	~~Clouds calculated~~Cloud data from 0.5° AM3 using 1.4° NCEP (~~U,V~~u,v). (0.5ºx0.5º) 2013 Aug 16	Fast-J v6.4, liquid cloud C1 (12 μm) and ice clouds per Fast-J, Briegleb averaging	Donner et al., 2011; Naik et al., 2013; Mao et al., 2013; Li et al., 2018; Lin et al., 2012.
GISS	GISS Model ~~2e1~~2E1	Clouds from climate model nudged to MERRA fields (2.5ºx2.0º) 2013 Aug 16	Fast-J2.	Schmidt et al., 2014; Shindell et al., 2012; Rienecker et al., 2011.
GMI	GSFC GMI	Cloud ~~fraction, liquid and ice water,~~CF+OD from MERRA-2 (1.3ºx1.0º) 2016 Aug 16	Fast-J v6.5, ~~single column,~~ liquid cloud C1 (6 μm) and ice cloud hexagonal (50 μm), Briegleb averaging	Strahan et al., 2013; Duncan et al., 2007.
IFS	ECMWF IFS	Cloud ~~fraction, liquid and ice water,~~data from IFS (0.7ºx0.7º) 2016 Aug 15	Williams et al. (2012). Liquid cloud (4-16 μm, using CCN), ice clouds ~~(Sun, 2001),~~ random overlap.	Flemming et al., 2015; Sun and Rikus, 1999; Sun, 2001.
MOCA	MOCAGE	Cloud ~~fraction, liquid water,~~data from ARPEGE operational analysis, ~~every~~ 3 ~~hours~~h. (1.0ºx1.0º) 2017 Aug 16	~~Photolysis are scaled following~~From Brasseur et al, (1998), using ~~cloud fraction~~CF and liquid water (10 μm), Briegleb averaging.	Guth et al., 2016; Arteta & Flemming, 2015
NCAR	CESM	Clouds ~~are re-computed with~~from CAM5 physics on MERRA ~~fields (U,V~~ (u,v,T, …). (0.6ºx0.5º) 2008 Aug 16	TUV lookup ~~photolysis~~ J-tables, scaled using ~~cloud fraction~~CF and liquid water content; Briegleb averaging.	Tilmes et al., 2016; Madronich, 1987
UCI	UCI CTM	Cloud ~~fraction, liquid and ice water,~~data from IFS T159L60N160 forecasts by U. Oslo. (1.1°x1.1°) 2005 Aug 16	Cloud-J v7.3, quadrature column atmospheres from decorrelation length. Liquid and ice clouds per Fast-J.	Neu et al., 2007; Holmes et al, 2013; Prather 2015; Prather et al., 2017
UKCA	UKCA	Cloud ~~fraction, liquid and ice water,~~data from UK Unified Model (1.9°x1.3°) 2008 Aug 17	Fast-J v6.4, cloud optical depths per Telford et al (2013). Briegleb averaging.	Morgenstern et al 2009; O'Connor et al 2014; Walters et al 2017.
UCIb	UCI CTM	same as UCI	Cloud-J v7.3, single column, Briegleb averaging.	~~ibid~~
Cloud data includes: cloud fraction (CF), in-cloud ice/liquid water path and effective radius, or in-cloud ice/liquid optical depth (OD in the visible).				

*Fast-J versions here based on Bian and Prather (2002) with updates, including standard tables for cloud optical properties and simplified estimate of effective radius. Cloud C1 refers to Deirmendjian liquid cloud size distribution from the Fast-J data tables (Wild et al., 2000).

**Briegleb's (1992) method approximates maximum-random overlap with a single column atmosphere and adjusted effective cloud fraction such that the cloud optical depth in the grid cell is COD(in-cell) = COD(in-cloud) x $CF^{3/2}$.

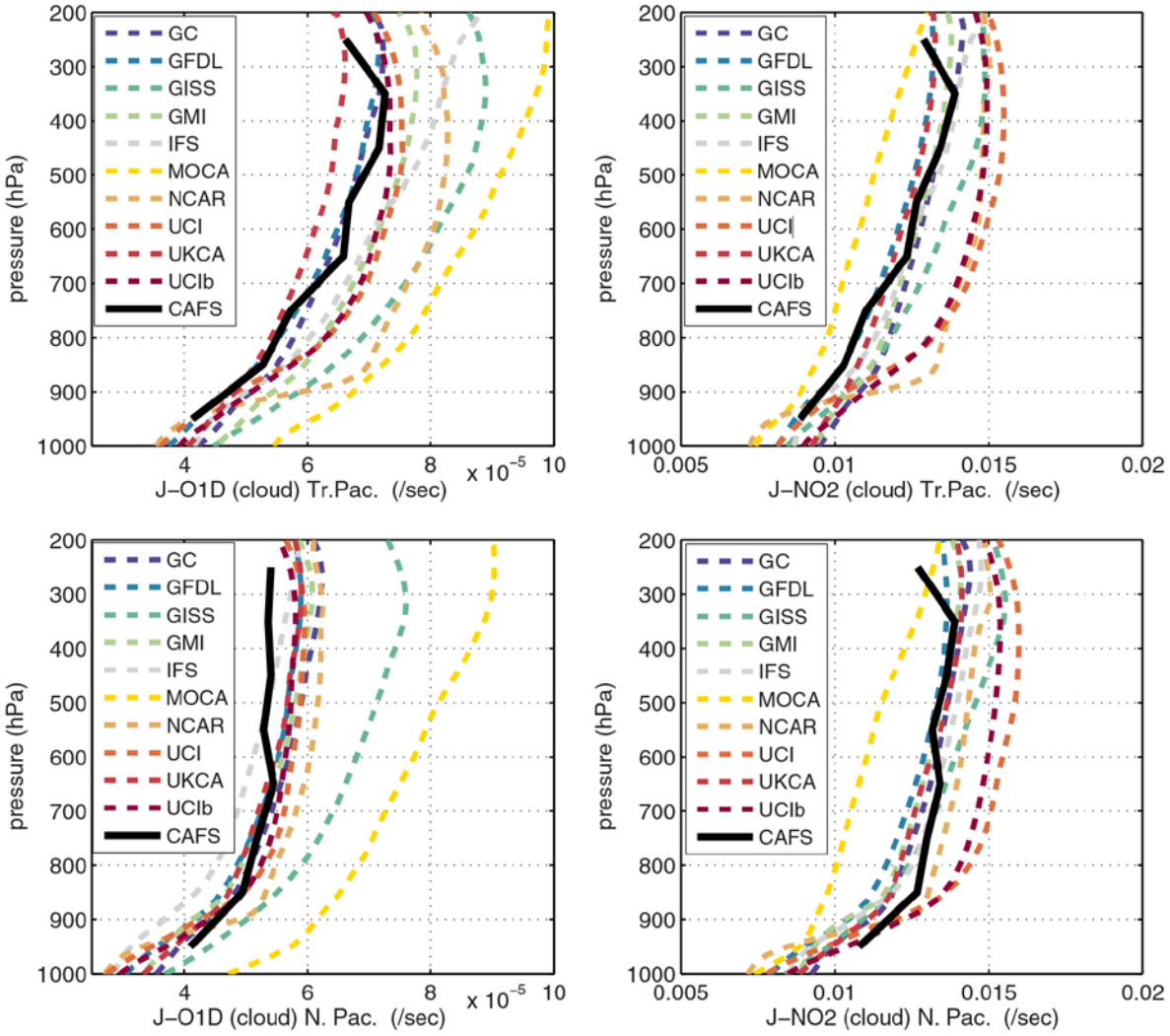

Figure 1. Profiles of all-sky ('cloudy') J-O1D and J-NO2 for the Tropical and North Pacific blocks. See Figures S2 and S3. The CAFS values are directly measured in ATom-1. The 10 models are sampled over 24 hours from ~~1~~a day in mid-August, selecting for cos(SZA) > 0.8. The UCI and UCIb models are distinct here because they treat overlapping clouds differently (cloud quadrature versus B-averaged cloud).

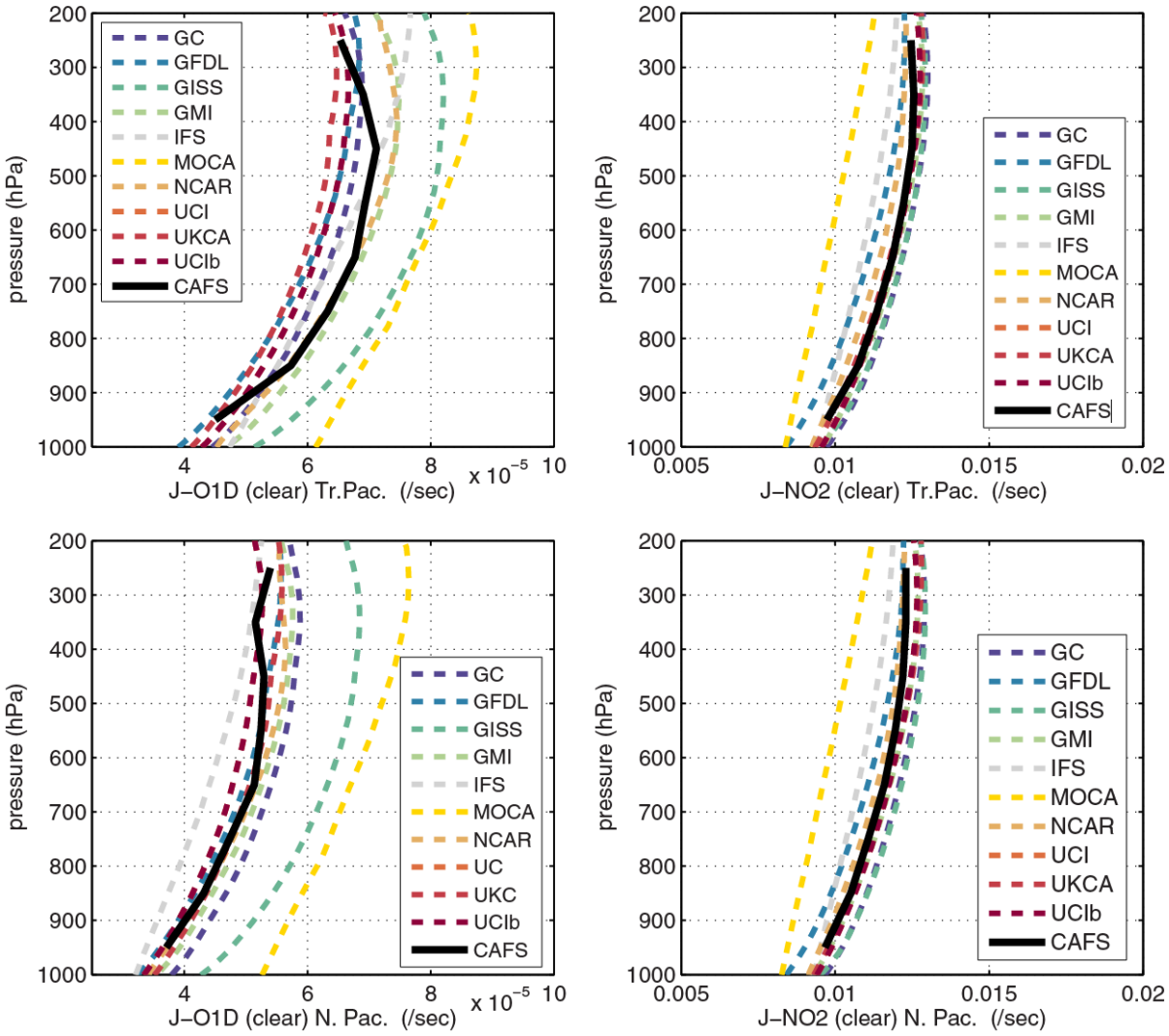

Figure 2. Profiles of clear-sky J-O1D and J-NO2 for the Tropical and North Pacific blocks. See Figure 1. CAFS here refers to TUV J's modeled at each point along the flight path. The UCI and UCI models are not separable since both have the same clear-sky J's. The spread in J-NO2 is likely due to different choices for interpolating cross sections and quantum yields. The J-O1D spread may be caused by the different ozone columns in the tropics, see Figure S3.

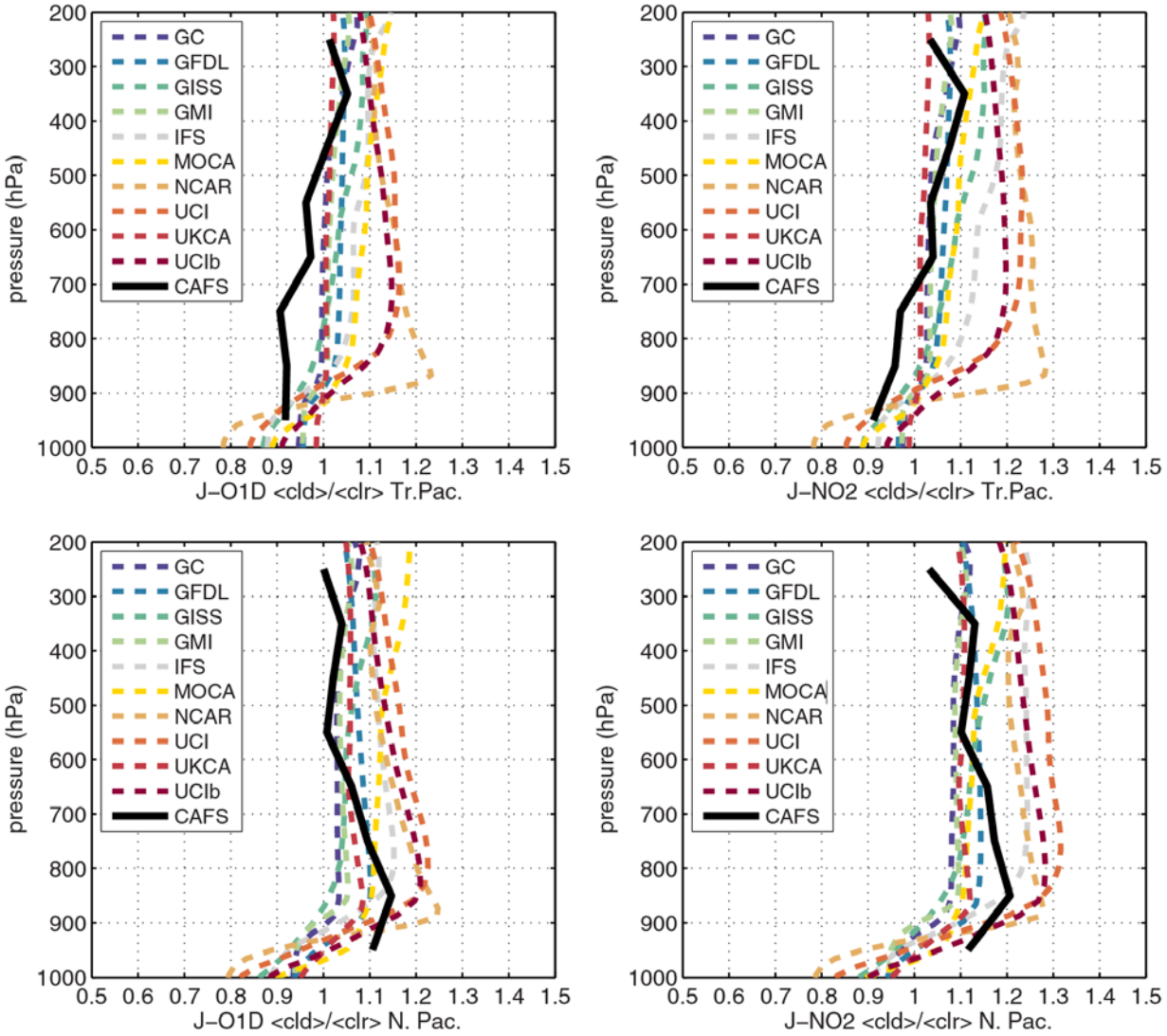

Figure 3. Profiles of the ratio of the average of J-cloudy to the average of J-clear for J-O1D and J-NO2 and for the 2 Pacific blocks. See Figures 1 and 2.

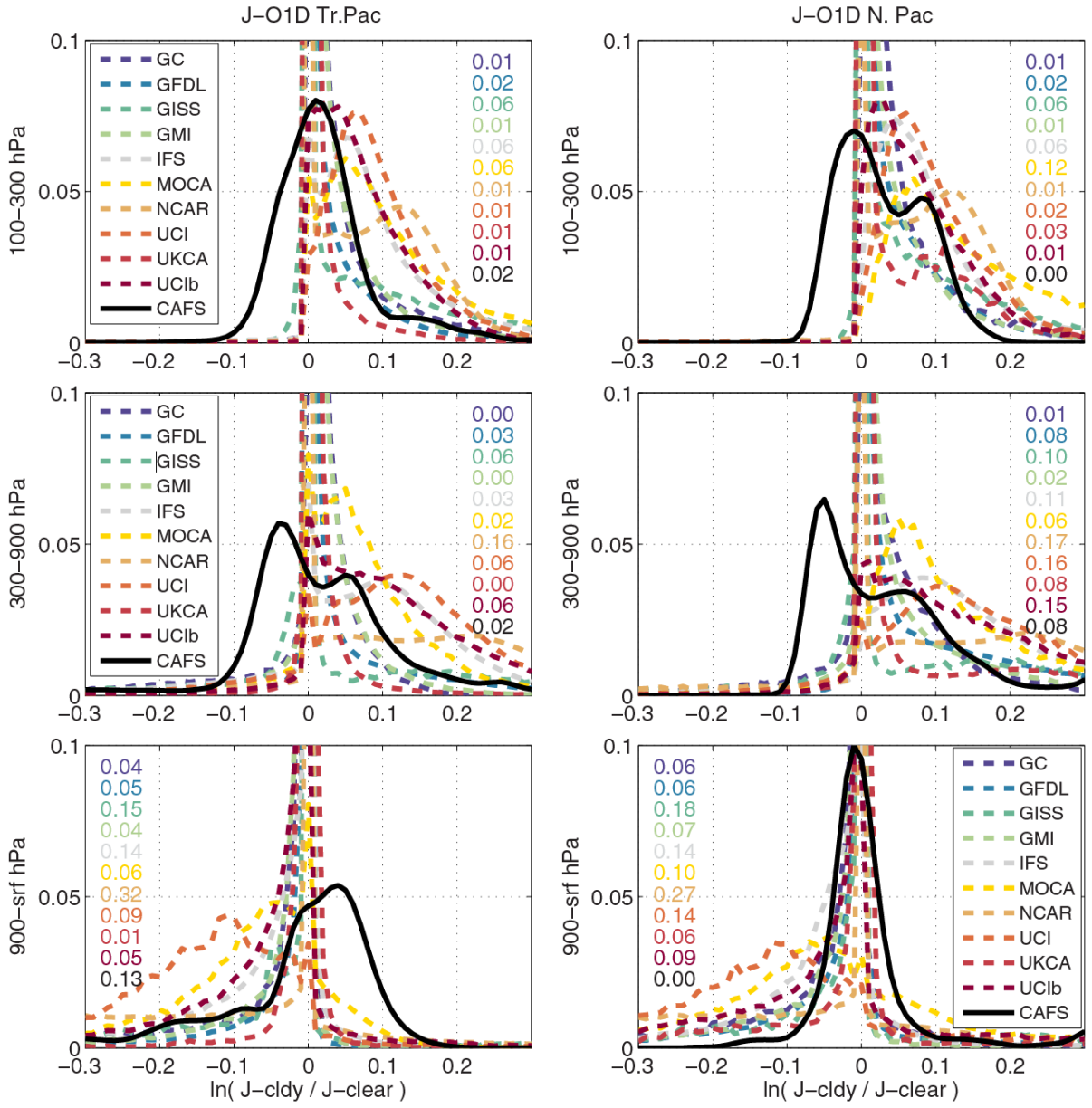

Figure 4a. Probability distribution of the natural log of the ratio of cloudy-to-clear J-O1D values (rlnJ) from 10 models ~~for a day in August~~ and from CAFS during ATom-1. The columns correspond to the 2 geographic blocks (Tropical Pacific, 20 ºS – 20 ºN x 160 ºE – 240 ºE, and North Pacific, 20 ºN – 50 ºN x 170 ºE – 225 ºE). The rows are the 3 pressure layers (100 – 300, 300 – 900, 900 – surface hPa). All histograms sum to 1, but for many models the peak values about rlnJ = 0, corresponding to cloud-free skies, are truncated. Where a significant fraction of events does not fit within the ±0.3 range – on the high side for 100 – 900 hPa and low side for 900 – surface hPa – the column of numbers, placed on the appropriate side and color coded to the legend, gives the fraction of occurrences outside the range.

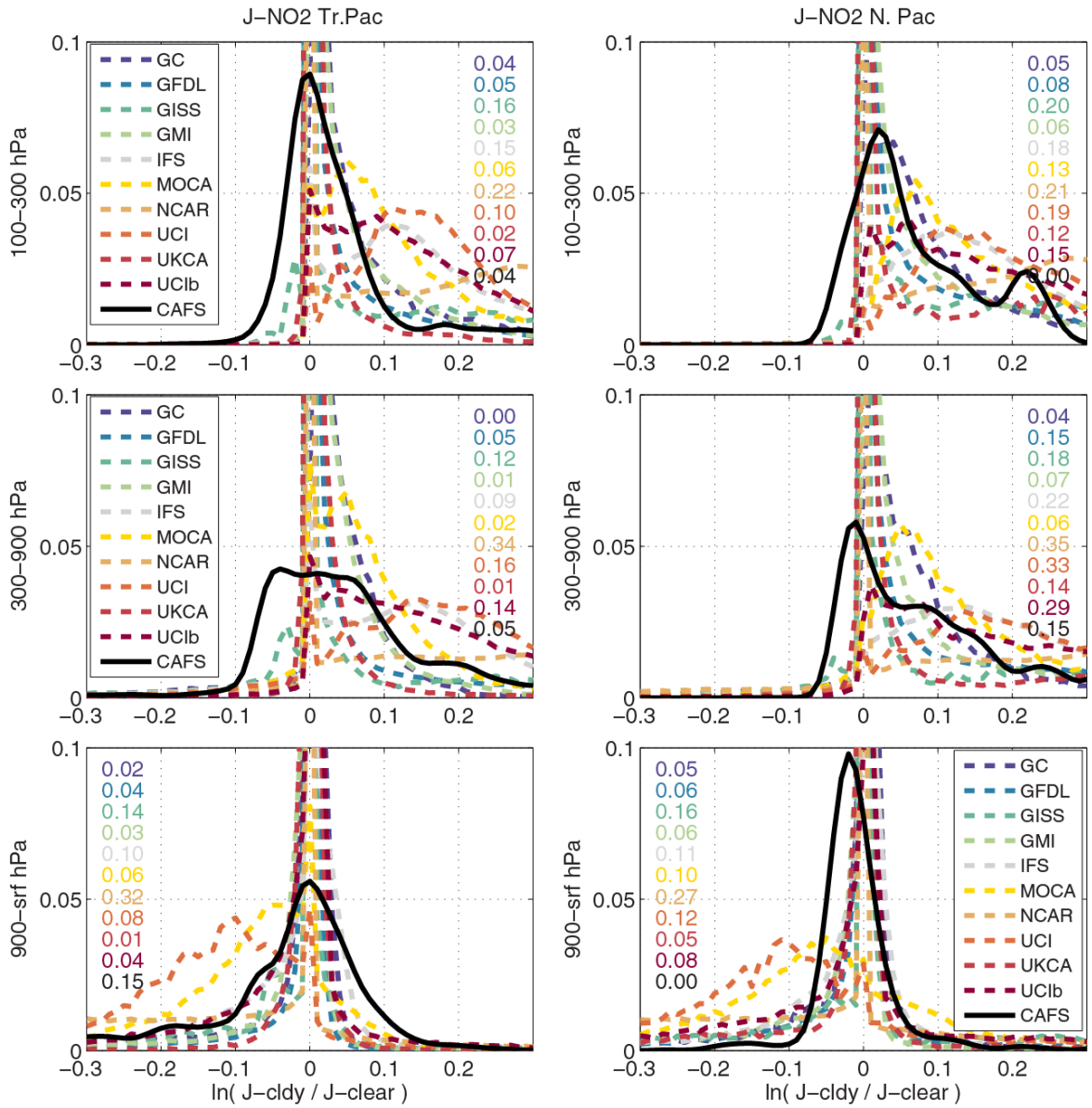

Figure 4b. Probability distribution of the natural log of the ratio of cloudy-to-clear J-NO2 values (rlnJ) from 10 models ~~for a day in August~~ and from CAFS during ATom-1. See Figure 4a. In general, J-NO2 is more response to clouds than is J-O1D.

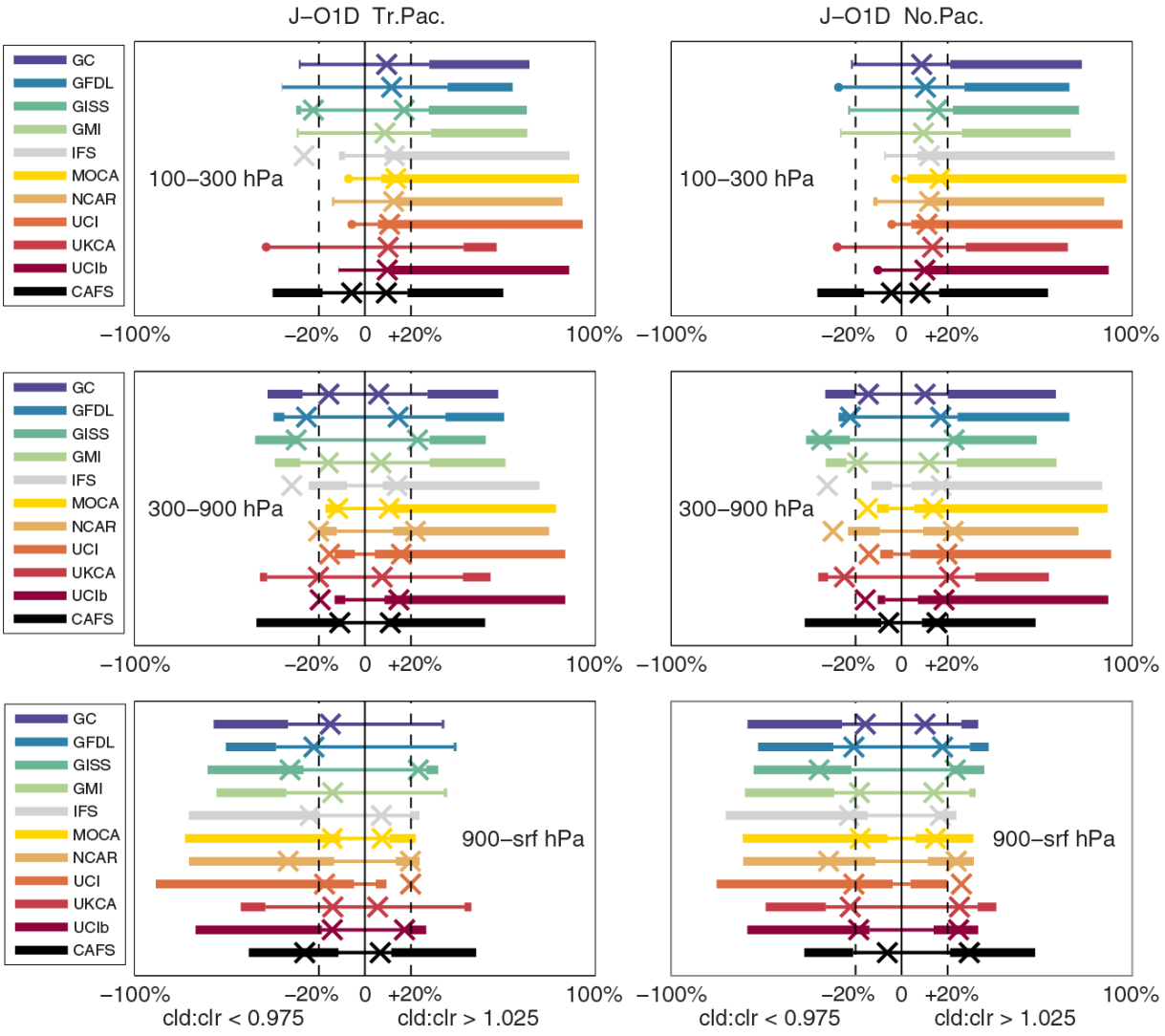

Figure 5a. Frequency of occurrence and magnitude of change in J-O1D caused by clouds. The panels and data sources are the same as in Figure 4ab. The horizontal lines all have length 1 and show the fraction of (i) cloud-~~reduced~~diminished J's (thick left segment, cloudy:clear ratio < 0.975), (ii) nearly cloud-free J's (thin central segment, 0.975 < ratio < 1.025), and (iii) cloud-enhanced J's (thick right segment, ratio > 1.025). Each line is plotted with its nearly-cloud-free segment centered on 0. The mean magnitude of ~~reduction~~diminishment/enhancement corresponding to the thick line segments is plotted as an 'X' on each line segment, using the X-axis [-1, +1] as the natural log of the cloudy:clear ratio. Ratio changes of -20 % and +20 % are shown as dashed vertical grid lines. The 'X's are not shown when the frequency of occurrence of either thick segment is < 0.02. For an example of how to read these figures consider the panel in row 3 column 1 (J-O1D, Tr. Pac, 900 – srf). The GFDL model has about 22 % cloud-~~reduced~~diminished J's (left segment) with an average value of 22 % below clear-sky J's (the 'X' on the left side); most of the remaining, 76 %, are nearly cloud-free (central thin segment). The GISS model has (from left to right) 42 % cloud-~~reduced~~diminished J's, 53 % cloud-free J's and only 5% cloud-enhanced J's for a total of 100 %; the cloud-~~reduced~~diminished J's average about 28 % less than clear-sky J's (the 'X' on the left) while the cloud-enhanced J's average about 22 % greater (the 'X' on the right side). See legend in Figure 5b.

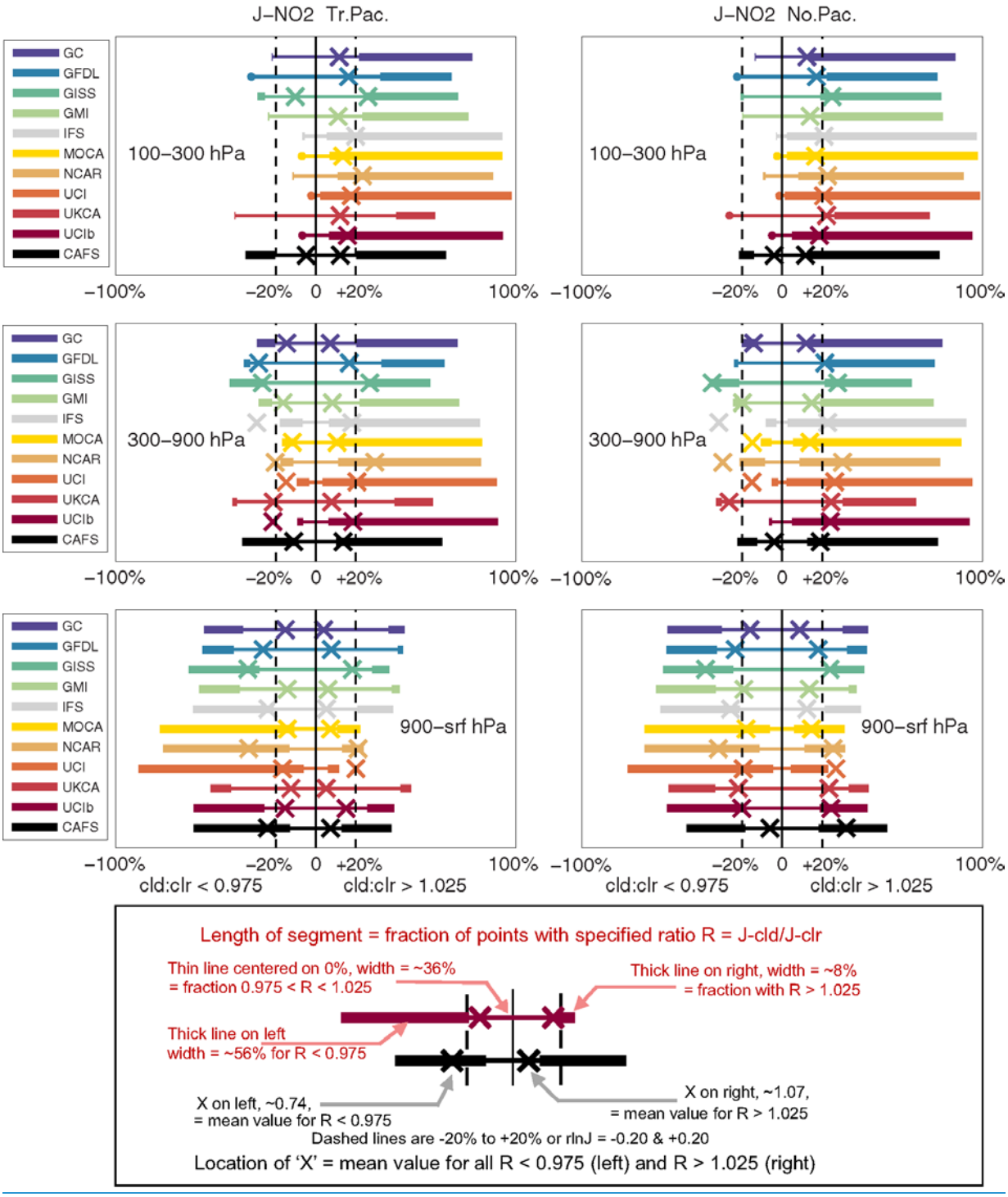

Figure 5b. Frequency of occurrence and magnitude of change caused by clouds in J-NO2. See Figure 5a.

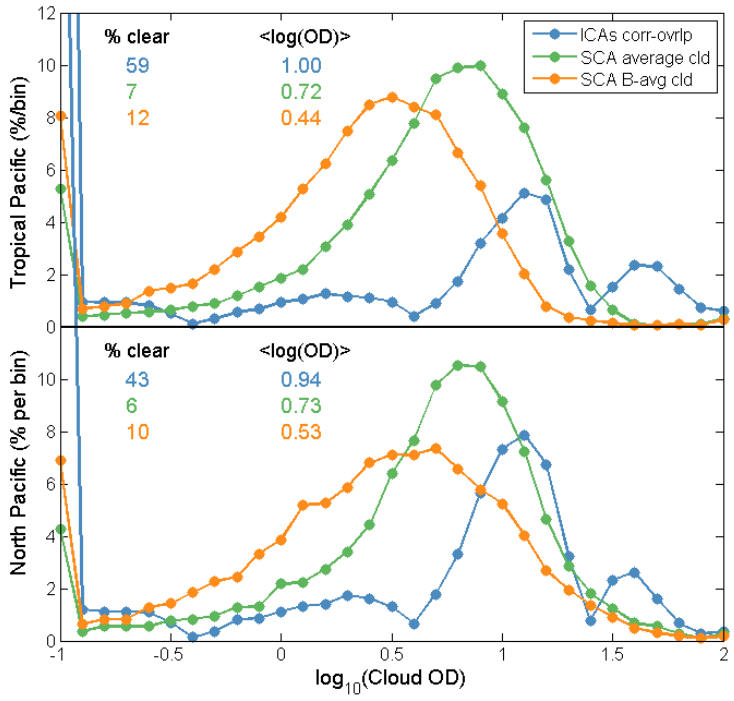

Figure 6. Histogram (% per 0.1 bin) in log of the total cloud optical depth (COD) based on method of implementing fractional clouds~~.~~: Cloud-J independent column atmospheres (ICAs, blue dots); simple cloud averaging over each cell (COD x CF, green dots) and B-averaging (COD x $CF^{3/2}$, orange dots). The 600-nm COD for two large regions (Tropical Pacific, 20 ºS – 20 ºN x 160 ºE – 240 ºE, and North Pacific, 20 ºN – 50 ºN x 170 ºE – 225 ºE. is collected for 16 Aug 2016 from eight 3-hour averages of COD and cloud fraction (CF) in each model layer. The "% clear" is the sum of fractions (%) with $\log_{10}$(total COD) < -0.5; and the "<log(OD)>" is the average of $\log_{10}$(total COD) > -0.5. The ~~UCI met~~cloud fields ~~are based on~~come from the ECMWF IFS cycle 38 system run at T159L60N160 resolution. ~~The UCI CTM uses a vertical de-correlation length (see Prather, 2015) to describe cloud overlap and, for each grid cell, generates a number of independent column atmospheres (ICAs), which are then mapped onto 4 quadrature column atmospheres (QCAs) representing 4 domains in $\log_{10}$(total COD): < -0.3; -0.3 to 0.6; 0.6 to 1.5; > 1.5.~~ On average the number of ICAs per cell in the tropical block is about 170, although individual cells may have >1000. ~~This histogram (blue dots) is our best estimate of the distribution of total COD from a 1D nadir perspective. The UCI J-values are calculated as the average over 4 quadrature column atmospheres (QCAs). In spite of the high, 40-60 % fraction of "clear" columns, the quadrature-averaged J-values from the UCI model in Figure 4 usually include some cloudy fraction. Thus the probability distribution of J-cloudy/J-clear using Cloud-J shows a peak frequency on the "cloudy" side (ratio >1, see text). The two single-column atmosphere (SCA) models use simple averaging (COD*CF, green dots) and B-averaging (COD x $CF^{3/2}$, orange dots) whereby the cloud fraction is reduced to approximate the cloud overlap. In these cases, a single J-value calculation is made with the SCA. B-averaging (Briegleb, 1992) is a parametric fix that appears to reduce the errors in simple CF-averaging while maintaining just one SCA. It is an improvement, but overall still underestimates J-values above 4 km and overestimates them below (See Figure 3 of Prather, 2015). Note that the SCA averaging dramatically reduces the "clear" fraction from ~50 % to ~10 %. It also reduces the average $\log_{10}$(total COD) from ~1 (ICAs) to 0.7 (SCA avg) to 0.5 (SCA B-avg). With either SCA method, there are just many more total COD in the range 0.5 to 10 ($\log_{10}$ from -0.7 to 1.0).~~In spite of the high, 40-60 % fraction of "clear" columns, the quadrature-averaged J-values usually include some cloudy fraction.

Supplementary Material for

Cloud impacts on photochemistry: building a ~~new~~ climatology of photolysis rates from the Atmospheric Tomography mission

Samuel R. Hall[1], Kirk Ullmann[1], Michael J. Prather[2], Clare M. Flynn[2], Lee T. Murray[3], Arlene M. Fiore[4,5], Gustavo Correa[4], Sarah A. Strode[6,7], Stephen D. Steenrod[6,7], Jean-Francois Lamarque[1], Jonathon Guth[8], Béatrice Josse[8], Johannes Flemming[9], Vincent Huijnen[10], N. Luke Abraham[11,12], Alex T. Archibald[11,12]

[1] Atmospheric Chemistry, Observations and Modeling Laboratory, National Center for Atmospheric Research, Boulder, CO 80301, USA
[2] Department of Earth System Science, University of California, Irvine, CA, USA
[3] Department of Earth and Environmental Sciences, University of Rochester, Rochester, NY, USA
[4] Department of Earth and Environmental Sciences, Columbia University, NY, NY, USA
[5] Lamont-Doherty Earth Observatory of Columbia University, Palisades, NY, USA
[6] NASA Goddard Space Flight Center, Greenbelt, MD, USA
[7] Universities Space Research Association (USRA), GESTAR, Columbia, MD, USA
[8] Centre National de Recherches Météorologiques, CNRS-Météo-France, UMR 3589, Toulouse, France
[9] European Centre for Medium-Range Weather Forecasts, Reading, UK
[10] Royal Netherlands Meteorological Institute, De Bilt, the Netherlands
[11] Department of Chemistry, University of Cambridge, Cambridge, U.K.
[12] National Centre for Atmospheric Science, U.K.
Correspondence to: Michael J. Prather (mprather@uci.edu)

Contents of this file

This Supplementary Material includes figures and tables referenced in the main text and useful for understanding this work, but not essential to its findings.

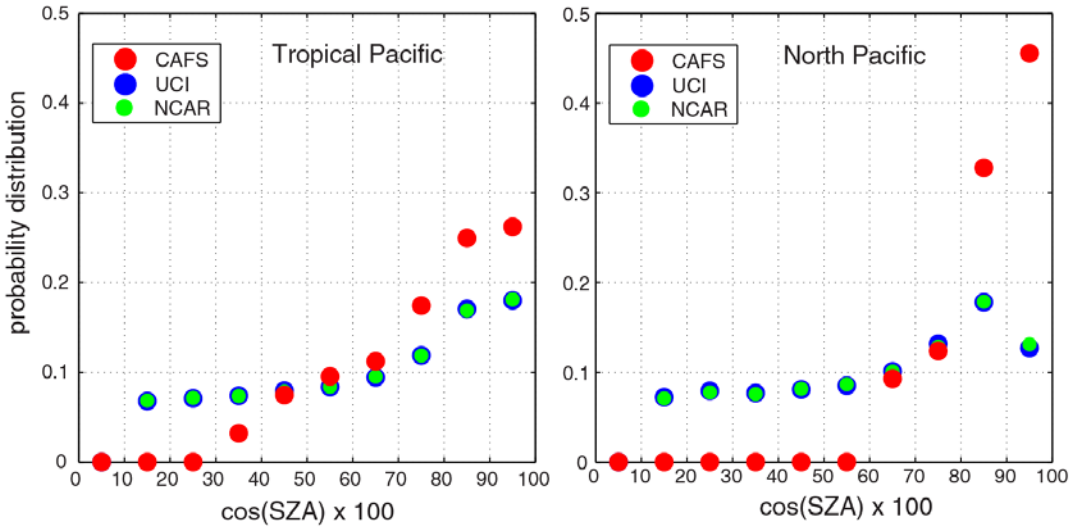

Figure S1. The probability distribution of solar zenith angles (SZAs) as sampled by ATom with the CAFS instrument (red) and by two models (UCI & NCAR) using regular sampling over the two geographic blocks: (1, left) Tropical Pacific and (2, right) North Pacific. The points represent the relative number of samples in each 0.10 interval of cos(SZA). ATom flights in this region were generally centered about noon, and hence CAFs has a higher proportion of high cos(SZA) values. For most of the analysis here only J's with cos(sza) > 0.8 are used, and with this restriction the number of CAFS measurements is 11,504 (block 1) and 4,867 (block 2). For UCI the number of points is 240,000 (block 1) and 120,000 (block 2); while for the higher resolution NCAR model, the values are 1,400,000 and 700,000, respectively.

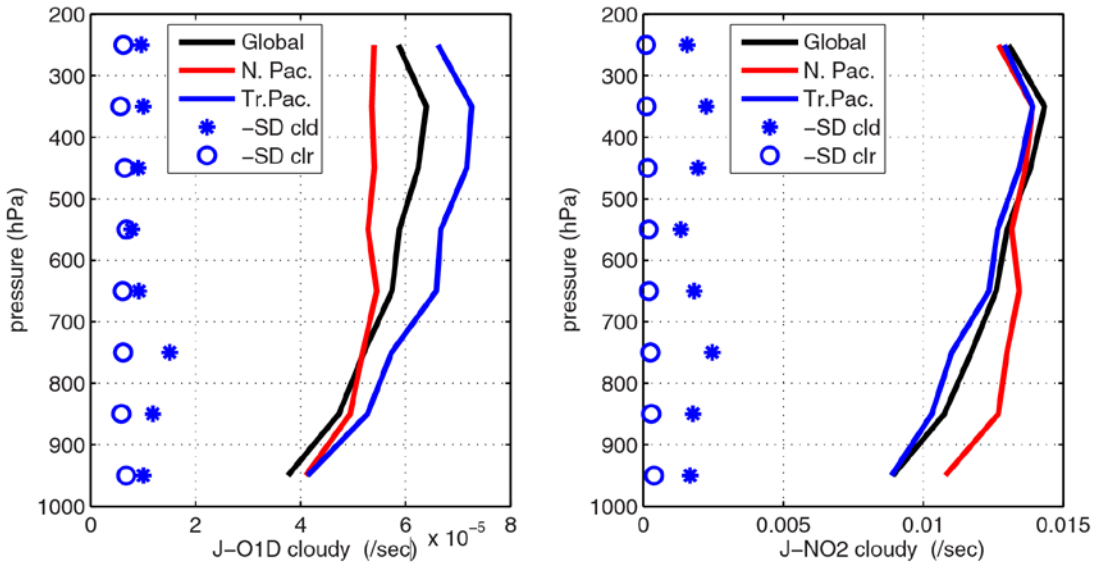

Figure S2. Mean CAFs profiles of J-O1D (left) and J-NO2 (right) from ATom-1 made under all-sky conditions for high-sun conditions, cos(sza) > 0.8. The 3 geographic blocks shown here are the standard blocks 1 (blue, Tropical Pacific, 20 ºS – 20 ºN x 160 ºE – 240 ºE), and 2 (red, North Pacific, 20 ºN – 50 ºN x 170 ºE – 225 ºE, plus a global block (black, 55 ºS – 55 ºN, all longitudes, including the Atlantic). Each 3-sec observation is averaged with equal weight in 100-hPa pressure bins. The standard deviation for block 1 (blue, *) is shown along with that from the corresponding TUV model calculation for clear sky (blue, o). The patterns here are expected: J-O1D is sensitive to O_3 absorption and hence has higher upper-tropospheric values in the tropics; J-NO2 is more sensitive to cloud scattering and hence has higher values in the ~~in the~~ lower troposphere of the North Pacific. The standard deviations show that J-O1D variance is driven by O_3 and SZA, and not by clouds; while the J-NO2 shows the opposite.

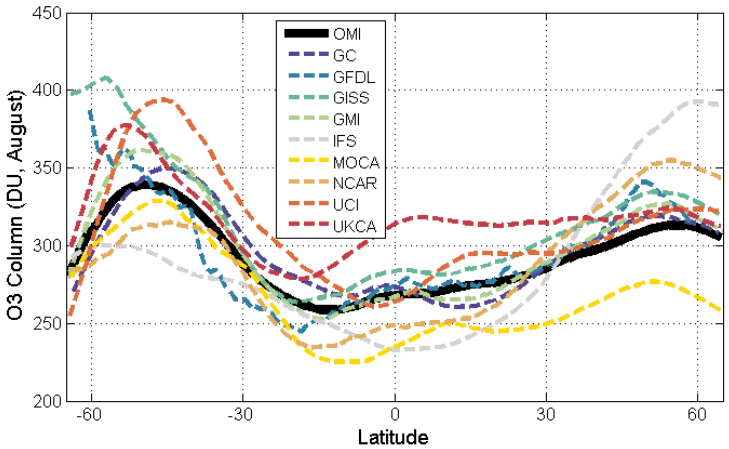

Figure S3. Total ozone columns (in DU) versus latitude in August for 9 models and 8 years of OMI observations (2010-2017, Levelt et al., 2006; Veefkind et al., 2006). Most curves are the monthly zonal means, but some data are from a single day, or just the ATom flight track for several days (e.g., GFDL, explains the lack of smoothness). Differences here can explain only some of the spread in clear-sky J-O1D values in Figure 2.

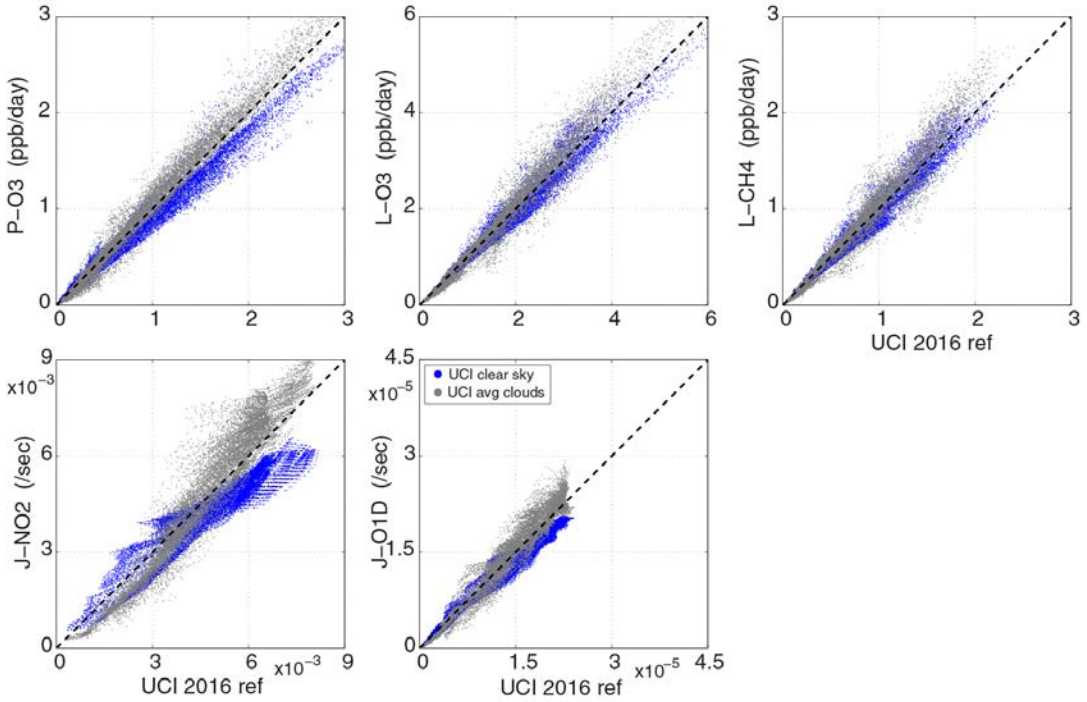

Figure S4. Effects of clear sky (blue points), simple averaged clouds (gray points), and fractional cloud overlap (the reference case, 1:1 dashed line) using the UCI CTM. X-axis is the same as the Y-axis, but for the reference model UCI 2016. Direct parcel-by-parcel comparison of modeled 24-hour reactivities (top row: P-O3, L-O3, L-CH4; all ppb/day) and photolysis rates (J-NO2, J-O1D; all /sec) calculated for a data stream of 14,880 simulated air parcels from 60 ºS to 60 ºN, 0.5 km to 12 km altitude, and along 180 ºW, see Prather et al., 2018. Each point is an average of the 5 simulated dates in August (8/01, 8/06, 8/11, 8/16, 8/21). UCI 2016 ref uses full cloud quadrature and the newly implemented decorrelation lengths for cloud overlap (Prather, 2015). From the figure, the different cloud treatments are clearly visible in the shifts in J-NO2 and J-O1D, and they have largest effect on P-O3 as compared with L-O3 and L-CH4. On average, the clear-sky simulation has 3-4% lesser J-values and similar changes in all 3 reactivities. The averaged-cloud method has about 12 % greater J-values (mostly above clouds), increasing reactivities by 5 % (L-O3 and L-CH4) to 10% (P-O3).

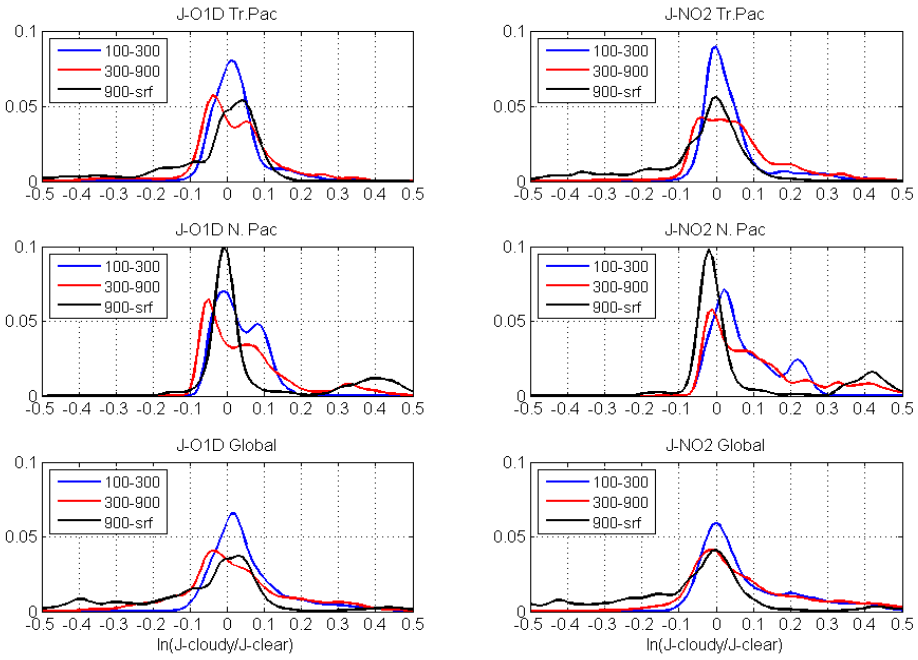

Figure S5. Histogram of the natural log of the ratio of cloudy-to-clear J values (J-O1D & J-NO2), designated rlnJ, which is calculated from the 10-sec CAFS data and sorted into 3 pressure bins (blue, 100 – 300; red, 300 – 900; black, 900 – surface hPa). Note that the upper level has a peak near 0.0, corresponding to clear sky; the lowest level extends more to values <0; and that the N. Pacific for <900 hPa has a large number of cloud enhanced J-values (rlnJ >0). The CAFS data were binned at 0.01 rlnJ and smoothed with a 1-2-1 filter six times.

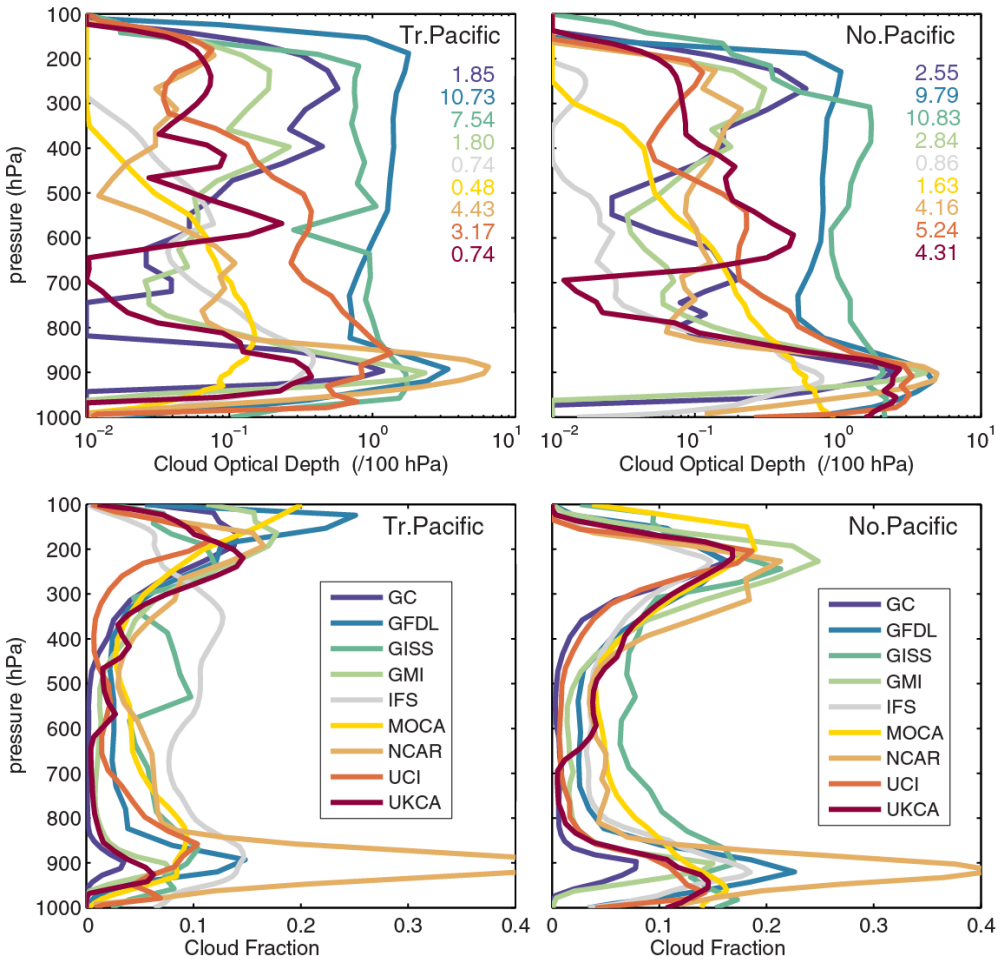

Figure S6. Averaged in-cell cloud optical depth (COD, at ~600 nm and per 100 hPa) and cloud fraction (CF) over the two geographic blocks studied here ~~blocks~~ (Tropical Pacific, 20 ºS – 20 ºN x 160 ºE – 240 ºE, and North Pacific, 20 ºN – 50 ºN x 170 ºE – 225 ºE). Averages are made over 24 hours for one day in mid-August as used in this paper. For these data (unlike the J-value statistics), all hours are weighted equally independent of solar zenith angle. Column total COD for each region is given in the order/color-indexed numbers on the right of each COD panel.

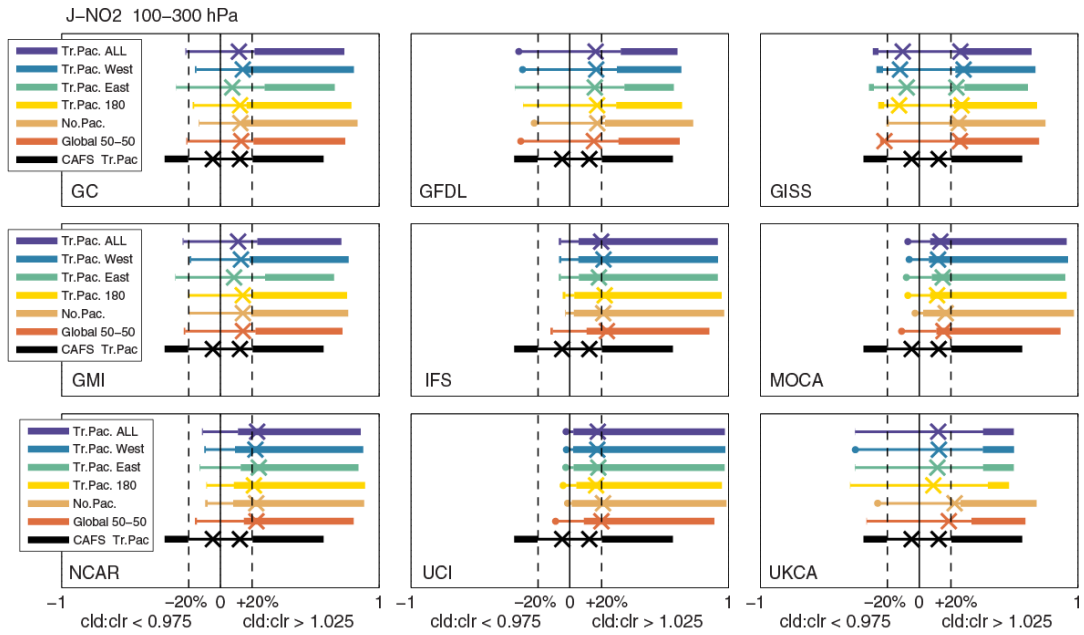

Figure S7a. The effect of sampling different regions of the tropical Pacific in terms of the frequency of occurrence and magnitude of changes caused by clouds in J-NO2 at 100-300 hPa. See Figure 5. Each of the 9 panels shows a single model with different sampling and also the CAFS observations over the tropical Pacific (bottom black bar and X's). The top purple bar is the entire tropical Pacific as defined in Figure 5 (20S-20N, 160E-240E) and the next three bars (blue, green, yellow) sub-sample this region into West (160E-200E), East (200E-240E) and 180E (175E-185E), respectively. The next two bars are the North Pacific (as in Figure 5) and a global sampling (50S-50N, all longitudes).

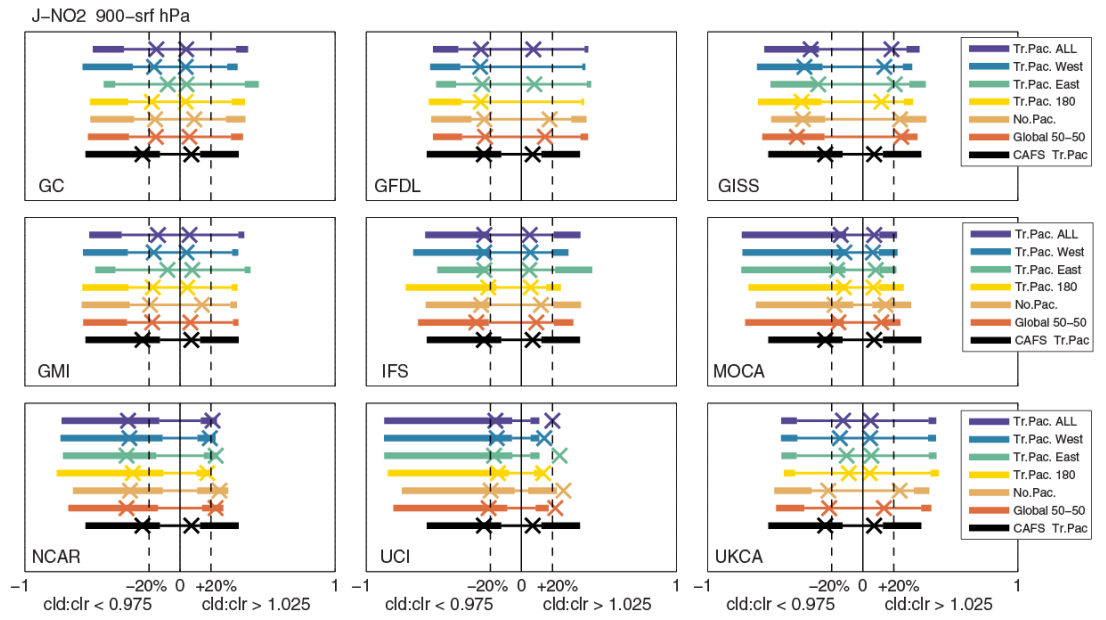

Figure S7b. The effect of sampling different regions of the tropical Pacific in terms of the frequency of occurrence and magnitude of changes caused by clouds in J-NO2 at surface-900 hPa. See Figure S7~~X~~a.

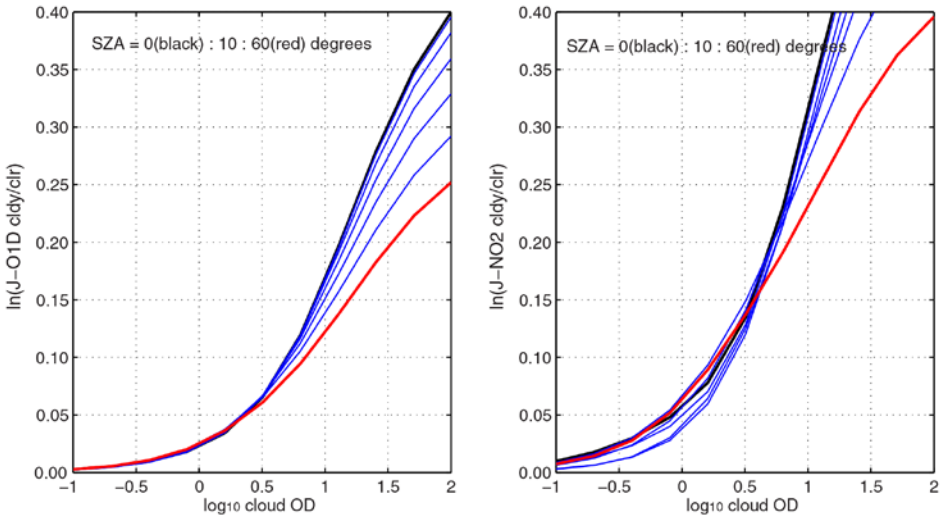

Figure S8~~7~~. The ratio of J-cloudy/J-clear calculated for J-O1D (left) and J-NO2 (right) at 300 hPa for a marine stratus cloud (CF = 100%) at about 900 hPa. The natural log of the ratio (rlnJ) is calculated for a cloud optical depth (COD) ranging from 0.1 to 100. The calculation uses Cloud-J (Prather, 2015), which does not scale COD, uses the truncated (order 8) phase function, and applies a constant lower boundary albedo = 0.05. The incident SZA ranges from 0º (black) to 60º (red) in 10º intervals (blue). The rlnJ's in this paper are restricted to 0º – 40º. A 5 % enhancement (rlnJ = 0.05) occurs at COD = 2 for J-O1D and COD = 1 for J-NO2, demonstrating the greater sensitivity of J-NO2 to clouds.

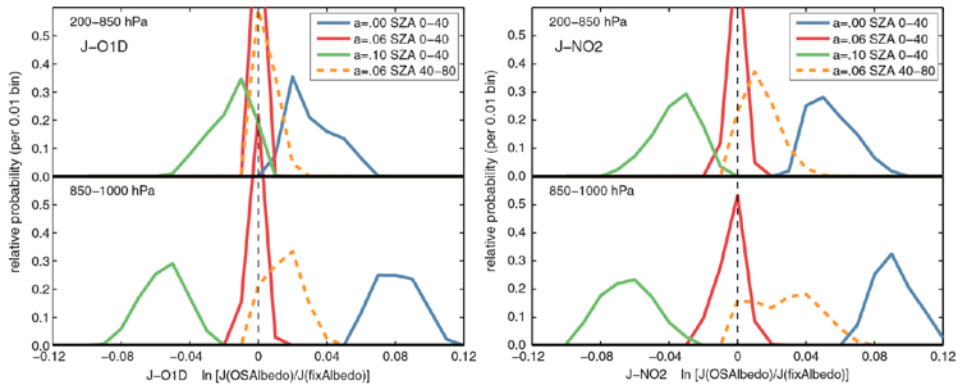

Figure S8~~9~~. Probability distribution of the natural log of the ratio of J-values calculated using an interactive ocean surface albedo (OSA) to J-values using a fixed albedo. J-O1D values (left) and J-NO2 values (right) assume clear skies for both OSA and fixed-albedo. This format is similar to Figure 4. The interactive OSA model includes a dependence on wavelength and incident-angle now in Cloud-J v8, see text. The fixed albedo is denoted by 'a =' in the legend. These distributions show the relative error in J-values calculated in typical models using a fixed albedo instead of the more physically based OSA models (Séférian et al., 2018). For both cases the reflected sunlight is assumed to be isotropic. The OSA depends on surface wind (sampled uniformly from 1 to 21 m/s) and chlorophyll abundance (sampled uniformly in log from 0.01 to 30 mg/m^3). The plots are also split between the lowermost troposphere (lower panels, >850 hPa) and free troposphere (upper, 200 – 850 hPa).

Table S1. Model contact information			
short name	long name	POCs for these simulations	
CAFS	---	Sam Hall <halls@ucar.edu>	Kirk Ullmann <ullmannk@ucar.edu>
GC	GEOSChem	Murray, Lee <lee.murray@rochester.edu>	
GFDL	GFDL AM3	Arlene Fiore <amfiore@ldeo.columbia.edu>	Gustavo Correa <gus@ldeo.columbia.edu>
GISS	GISS ModelE2	Murray, Lee <lee.murray@rochester.edu>	
GMI	GSFC GMI	Sarah A. Strode <Sarah.A.Strode@nasa.gov>	Stephen Steenrod <Stephen.D.Steenrod@nasa.gov>
IFS	ECMWF IFS	Johannes Flemming <johannes.flemming@ecmwf.int>	Vincent Huijnen <vincent.huijnen@knmi.nl>
MOCA	MOCAGE	Beatrice Josse <beatrice.josse@meteo.fr>	Jonathan Guth <jonathan.guth@meteo.fr>
NCAR	CESM	Jean-Francois Lamarque <lamar@ucar.edu>	
UCI	UCI CTM	Michael Prather <mprather@uci.edu>	Clare Flynn <claref@uci.edu>
UKCA	UKCA	Luke Aabraham <luke.abraham@atm.ch.cam.ac.uk>	Alex Archibald <ata27@cam.ac.uk>, Marcus Koehler <m.koehler@uea.ac.uk>